Cenozoic aridization in Central Eurasia shaped diversification of toad-headed agamas (*Phrynocephalus*; Agamidae, Reptilia)

Evgeniya N. Solovyeva[1], Vladimir S. Lebedev[1], Evgeniy A. Dunayev[1], Roman A. Nazarov[1], Anna A. Bannikova[2], Jing Che[3,4], Robert W. Murphy[3,5] and Nikolay A. Poyarkov[2]

[1] Zoological Museum, Lomonosov Moscow State University, Moscow, Russia
[2] Biological Faculty, Department of Vertebrate Zoology, Lomonosov Moscow State University, Moscow, Russia
[3] State Key Laboratory of Genetic Resources and Evolution, and Center for Excellence in Animal Evolution and Genetics, Kunming Institute of Zoology, Chinese Academy of Sciences, Kunming, Yunnan, China
[4] Southeast Asia Biodiversity Research Institute, Chinese Academy of Sciences, Yezin, Nay Pyi Taw, Myanmar
[5] Faculty of Arts and Science, Department of Ecology & Evolutionary Biology, University of Toronto, Toronto, ON, Canada

ABSTRACT

We hypothesize the phylogenetic relationships of the agamid genus *Phrynocephalus* to assess how past environmental changes shaped the evolutionary and biogeographic history of these lizards and especially the impact of paleogeography and climatic factors. *Phrynocephalus* is one of the most diverse and taxonomically confusing lizard genera. As a key element of Palearctic deserts, it serves as a promising model for studies of historical biogeography and formation of arid habitats in Eurasia. We used 51 samples representing 33 of 40 recognized species of *Phrynocephalus* covering all major areas of the genus. Molecular data included four mtDNA (*COI, ND2, ND4, Cytb*; 2,703 bp) and four nuDNA protein-coding genes (*RAG1, BDNF, AKAP9, NKTR*; 4,188 bp). AU-tests were implemented to test for significant differences between mtDNA- and nuDNA-based topologies. A time-calibrated phylogeny was estimated using a Bayesian relaxed molecular clock with nine fossil calibrations. We reconstructed the ancestral area of origin, biogeographic scenarios, body size, and the evolution of habitat preference. Phylogenetic analyses of nuDNA genes recovered a well-resolved and supported topology. Analyses detected significant discordance with the less-supported mtDNA genealogy. The position of *Phrynocephalus mystaceus* conflicted greatly between the two datasets. MtDNA introgression due to ancient hybridization best explained this result. Monophyletic *Phrynocephalus* contained three main clades: (I) oviparous species from south-western and Middle Asia; (II) viviparous species of Qinghai–Tibetan Plateau (QTP); and (III) oviparous species of the Caspian Basin, Middle and Central Asia. *Phrynocephalus* originated in late Oligocene (26.9 Ma) and modern species diversified during the middle Miocene (14.8–13.5 Ma). The reconstruction of ancestral areas indicated that *Phrynocephalus* originated in Middle East–southern Middle Asia. Body size miniaturization likely occurred early in the history of

Phrynocephalus. The common ancestor of *Phrynocephalus* probably preferred sandy substrates with the inclusion of clay or gravel. The time of Agaminae radiation and origin of *Phrynocephalus* in the late Oligocene significantly precedes the landbridge between Afro-Arabia and Eurasia in the Early Miocene. Diversification of *Phrynocephalus* coincides well with the mid-Miocene climatic transition when a rapid cooling of climate drove progressing aridification and the Paratethys salinity crisis. These factors likely triggered the spreading of desert habitats in Central Eurasia, which *Phrynocephalus* occupied. The origin of the viviparous Tibetan clade has been associated traditionally with uplifting of the QTP; however, further studies are needed to confirm this. Progressing late Miocene aridification, the decrease of the Paratethys Basin, orogenesis, and Plio–Pleistocene climate oscillations likely promoted further diversification within *Phrynocephalus*. We discuss *Phrynocephalus* taxonomy in scope of the new analyses.

INTRODUCTION

Historical biogeography aims to understand the drivers of speciation including the roles played by plate tectonics and climatic change (*Lomolino et al., 2006*). The eastern part of the Great Palearctic Desert Belt spans from Eastern Europe to Eastern China, including Middle Asia (Kazakhstan, Kyrgyzstan, Uzbekistan, Tajikistan, and Turkmenistan) and Central Asia. Middle and Central Asia have one of the oldest desert areas. Desertification started at least 23.8–22.0 million years ago (Ma) (*Xia & Hu, 1993*; *Guo et al., 2002*). Various paleogeographic factors played major roles in the shifting of Central Eurasian climate (*Ramstein et al., 1997*). These include the Miocene retreat of the Paratethys Sea, which stretched over Eurasia 30 Ma (*Popov et al., 2004*, *2009*), tectonic activity in Southwest Asia (*Whiteman, 1978*; *Weise, 1974*; *Macey et al., 1993*; *Golonka, 2004*), and the uplifting of the Qinghai–Tibetan Plateau (QTP; *Harrison et al., 1992*, *1995*; *Ramstein et al., 1997*; *Zhisheng et al., 2001*; *Molnar, 2005*). Aridization led to the disappearance of forests and formation of desert ecosystems (*Cerling et al., 1997*; *Ma et al., 1998*) and it intensified in the late Cenozoic following the formation of Asian monsoon climate (*Guo et al., 2002*).

Central Eurasian deserts cradle a rich herpetofauna (*Chernov, 1948*, *1959*; *Likhnova, 1992*; *Ananjeva & Tuniev, 1992*; *Szczerbak, 2003*). In the late Cenozoic, dramatic climatic changes influenced the origins, diversification and distribution of Central Eurasian reptiles (*Macey et al., 2000*; *Melville et al., 2009*). However, the dearth of phylogenetic and historical biogeographic studies for Central Eurasia does not allow the testing of hypotheses on the biological consequences of Cenozoic climatic events. The reptile fauna of the Central Asian deserts is particularly diverse, yet we still have limited understanding of the drivers of evolution of the constituent species (*Melville et al., 2009*).
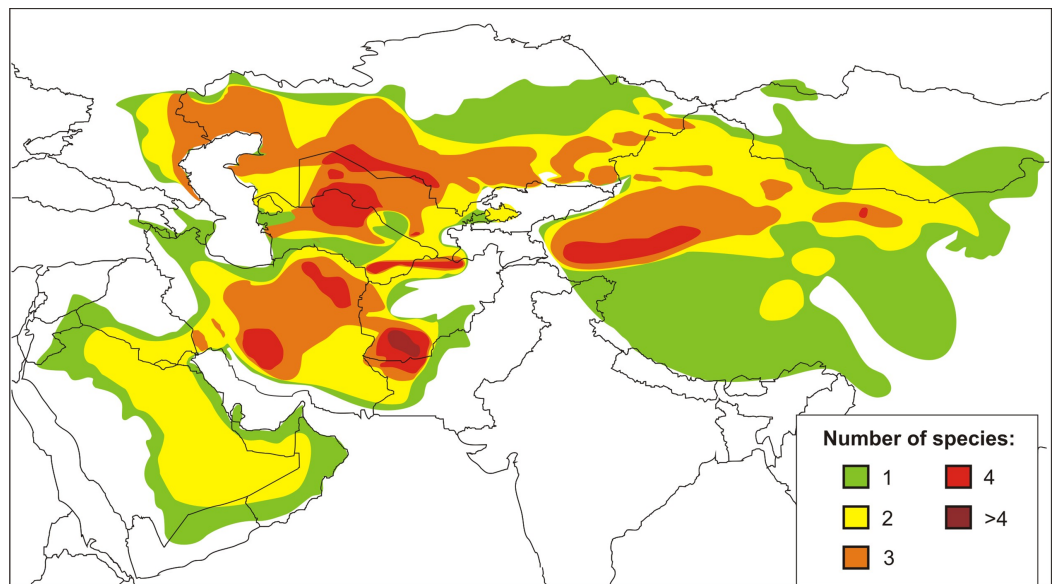
Figure 1 Current distribution and species richness of the genus *Phrynocephalus.* Color indicates the number of sympatric species of *Phrynocephalus* (from one to over four).

Full-size 🖼 DOI: 10.7717/peerj.4543/fig-1

The agamid genus *Phrynocephalus* Kaup, 1825, or toad-headed lizards, is one of the most speciose genera in its family. It contains from 28 to over 42 species and spans arid regions from northwestern China to the western side of the Caspian Sea, across the QTP, and Southwest Asia to the Arabian Peninsula (*Wermuth, 1967*; *Moody, 1980*; *Barabanov & Ananjeva, 2007*; *Guo & Wang, 2007*; *Uetz & Hošek, 2016*; *Kamali & Anderson, 2015*) (Fig. 1). The species are ecologically important components of the Central Eurasian desert fauna and are highly adapted to sand dunes and stony montane deserts from sea level up to 6,400 m a.s.l. (*Zhao, Zhao & Zhou, 1999*). They exhibit high levels of variation in ecological and morphological diversity, and the species range from being habitat generalists to specialists (*Clemann et al., 2008*; *Dunayev, 2009*). Oviparous reproduction occurs in lower elevations and yet viviparous species occur on the QTP (*Zhao & Adler, 1993*; *Pang et al., 2003*; *Guo & Wang, 2007*). The involvement of *Phrynocephalus* in so-called "substrate races" leads to much taxonomic confusion (*Dunayev, 2009*), especially because their phylogenetic relationships and historical biogeography remain uncertain. Considerable taxonomic, morphological, allozyme, karyological, osteological, and ethological research has been conducted on the charismatic *Phrynocephalus* of Central Asia (for a brief review on history of phylogenetic studies of the genus *Phrynocephalus* see Supplemental Information 1). Regardless the phylogenetic and taxonomic relationships within the toad-headed agamas remain controversial and largely unresolved (*Ananjeva & Tuniev, 1992*; *Arnold, 1999*; *Macey et al., 1993*; *Dunayev, 1996b*; *Golubev, 1993*; *Zhao & Adler, 1993*; *Pang et al., 2003*; *Ananjeva et al., 2006*; *Solovyeva et al., 2011*, *Solovyeva, Dunayev & Poyarkov, 2012*; and references therein). Hypothesis-testing can help deduce their origin, diversification and dispersal (*Guo & Wang, 2007*; *Melville et al., 2009*; *Solovyeva et al., 2014*). The most complete genealogic hypothesis obtained up to date

(*Solovyeva et al., 2014*) is based entirely on the mtDNA data; several major nodes of the tree have little or no support, so elaboration of a more robust phylogeny based on nuclear markers is needed.

Herein, we explore a number of unresolved questions by using both mitochondrial and nuclear DNA markers based for 36 species of *Phrynocephalus* that cover the entire range of the genus. Specifically, we pursue three main objectives: (1) test the hypothesis that the nuDNA and mtDNA trees give compatible estimations of historical relationships; (2) evaluate hypotheses concerning potential climatic and tectonic drivers of speciation by using time-tree ages of each lineage calibrated based on molecular dating and fossils; and (3) reconstruct the ancestral distributions to differentiate among competing scenarios of historical biogeography. Our work offers the most complete taxon sampling to date by including up to 70% of the diversity of the genus. It helps to resolve longstanding phylogenetic and biogeographic issues of Central Eurasian biogeography and provides insights into the biogeographic consequences of Cenozoic aridization.

MATERIALS AND METHODS

DNA samples

We used 51 samples representing 33 nominal species of *Phrynocephalus* from the collection of Zoological Museum of Moscow University (ZMMU). The primary outgroup included six other Agaminae species from the genera *Agama* Daudin, 1802, *Paralaudakia* Baig, Wagner, Ananjeva & Böhme, 2012, *Stellagama* Baig, Wagner, Ananjeva & Böhme, 2012, and *Trapelus* Cuvier, 1817 (Tables S1 and S2). For alcohol-preserved voucher specimens, muscle tissue was removed and preserved in 96% ethanol and stored subsequently at −35 °C; three tissue samples were obtained from the dried skin of voucher specimens.

DNA extraction, PCR conditions, and sequencing

Muscle and skin tissues were digested with Proteinase K and total genomic DNA was extracted using a standard phenol–chloroform extraction protocol followed with ethanol precipitation of DNA (*Sambrook, Fritsch & Maniatis, 1989*). Our analyses used the mitochondrial DNA dataset of *Solovyeva et al. (2014)*, which included the following four mtDNA gene fragments: 654 bp of *COI* (cytochrome oxidase subunit I), 1,053 bp of *ND2* (NADH-dehydrogenase subunit II), 705 bp of *ND4* (NADH-dehydrogenase subunit IV), and 297 bp of *Cytb* (cytochrome *b*). The total length of the concatenated mtDNA genes was 2,703 bp (Table S3). We also amplified exons of four nuclear DNA genes as follows: 1,455 bp of *RAG-1* (recombination activating gene), 675 bp of *BDNF* (brain derived neurotrophic factor), 1,182 bp of *AKAP9* (A-kinase anchor protein 9), and 876 bp of *NKTR* (natural killer-tumor recognition). The total length of these data was 4,188 bp (Table S3).

Primer pairs for PCR were taken from the literature (mtDNA: *Ivanova, DeWaard & Hebert, 2006*; *Wang & Fu, 2004*; *Macey et al., 2000*; *Arévalo, Davis & Sites, 1994*; *Pang et al., 2003*; nuDNA: *Shoo et al., 2008*; *Townsend et al., 2008, 2011*) or designed by us (Table S4). PCR amplifications were performed in a reaction volume of 20 µl containing ca. 100 ng of

template DNA, 0.3 pM/μl of each PCR primer, 1xTaq-buffer containing 25 mM MgCl$_2$ (Silex, Moscow, Russia), 0.2 mM dNTPs, and 1 unit of aq-polymerase (Silex, Moscow, Russia; 5 units/μl). Protocols for PCR amplification were provided in the Supplemental Information 2. PCR products were purified with alcohol precipitation and a PCR purification kit (Isogen, Moscow, Russia). Purified products were sequenced with both forward and reverse primers using ABI PRISM® BigDye™ Terminator v.3.1 reagents and an Applied Biosystems 3730 DNA Analyzer (Applied Biosystems, Carlsbad, CA, USA). All sequencing followed the manufacturer's protocols as given in the Engelgart's IMB RAN (Moscow, Russia). All unique sequences were deposited in GenBank (Tables S1 and S2).

Taxa selection and molecular data

We added six sequences of *Phrynocephalus* available in GenBank to the final alignments (Table S2). Thirty-seven agamid species were selected as outgroup taxa for phylogenetic inference and time-tree calibration. These included the following Near Eastern and Middle Asian genera closely related to *Phrynocephalus* (Agaminae: *Paralaudakia*, *Laudakia* Gray, 1845, *Trapelus*, *Stellagama*) as well as more distant Southeast Asian agamids (Draconinae: *Acanthosaura* Gray, 1831, *Draco* Linnaeus, 1758, *Calotes* Daudin, 1802; Leiolepidinae: *Leiolepis* Cuvier, 1829) and Australian taxa (Amphibolurinae: *Moloch* Gray, 1841, *Pogona* Storr, 1982, *Chlamydosaurus* Gray, 1825). The most distant outgroup taxa also included representatives of Chamaeleonidae, Phrynosauridae, Dactyloidae, Iguanidae, Corytophanidae, Tropiduridae, Polychrotidae, Leiocephalidae, Lacertidae, Opluridae, Crotaphytidae, including representative taxa of the following agamid genera: *Stellagama*, *Trapelus*, *Paralaudakia*, and *Agama* for both nuclear and mtDNA dataset, and additionally representative taxa of the genera *Xenagama* Boulenger, 1895, *Laudakia*, *Bufoniceps* Arnold, 1992, *Pseudotrapelus* Fitzinger, 1843 and *Calotes* for the mtDNA dataset. Details on taxonomy, GenBank accession numbers and associated references were summarized in Tables S1 and S2.

Phylogenetic inference

Sequences were first aligned using the Clustal W algorithm (*Thompson, Higgins & Gibson, 1994*) in BioEdit Sequence Alignment Editor 7.1.3.0 (*Hall, 1999*), with default parameters. Subsequently, the alignment was checked and manually revised if necessary using Seqman 5.06 (*Burland, 1999*). Genetic distances were calculated using MEGA 6.1 (*Tamura et al., 2013*).

Phylogenetic tree reconstructions were performed with the following data sets: (1) each nuclear gene separately; (2) all nuclear genes concatenated; (3) all nuclear genes combined in a species-tree estimation; (4) a concatenation of four mitochondrial genes as in *Solovyeva et al. (2014)* but with the addition of *Phrynocephalus rossikowi* Nikolsky, 1898. To test whether the inclusion of distant outgroups can introduce any bias into results of tree inference, the nuclear and mitochondrial concatenations were put through an additional set of reconstructions omitting all non-agamid and non-agamine taxa, respectively. The optimum partitioning schemes for nuclear and mitochondrial

alignments were identified with PartitionFinder (*Lanfear et al., 2012*) using greedy search algorithm under the AICc criterion.

Phylogenetic trees were reconstructed under the maximum likelihood (ML), maximum parsimony (MP), and Bayesian inference (BI) criteria. The ML trees were generated in Treefinder v.March 2011 (*Jobb, 2011*). For each subset, the best fitting substitution model was selected using the Bayesian Information Criterion in Treefinder. Nodal support was assessed by 1,000 bootstrap replications (BSP) and expected likelihood weights (ELW). The unweighted MP analyses were conducted in PAUP* v4.0b10 (*Swofford, 2002*) with 1,000 bootstrap replications. Bayesian inference was performed in MrBayes v3.1.2 (*Ronquist & Huelsenbeck, 2003*) with two simultaneous runs, each with four chains, for 200 million generations. We checked the convergence of the runs and that the effective sample sizes were all above 200 by exploring the likelihood plots using TRACER v1.5 (*Rambaut & Drummond, 2007*). The initial 10% of trees were discarded as burn-in. Confidence in tree topology was assessed by posterior probability (BPP) (*Huelsenbeck & Ronquist, 2001*).

Species-tree estimation was performed in *BEAST (*Heled & Drummond, 2010*) using the four independent nuclear loci. Prior to the analysis, the molecular clock assumption was tested separately for each exon by hierarchical likelihood ratio tests using PAML v4.7 (*Yang, 2007*). Following the results of these tests, we used a strict clock model for *BDNF* and uncorrelated lognormal relaxed clock models for the other three loci. No calibration information was utilized; the clock rate for *BDNF* was set to one. We used the same models and partitioning scheme as in the ML analysis. A Yule prior for the species-tree shape and the piecewise constant population size model were assumed. Default priors were used for all other parameters. Two runs of 500 million generations were conducted in BEAST v1.8.0 (*Drummond et al., 2012*). Parameter convergence was assessed in Tracer; the first 10% of generations were discarded as the burn-in. TreeAnnotator v1.8.0 (part of the BEAST package) was used to generate the maximum clade credibility tree.

Partition homogeneity test (*Farris et al., 1994*, *1995*) as implemented in PAUP* v4.0b10 (*Swofford, 2002*) was used to ensure the absence of significant conflict among the four nuclear datasets (*p*-value = 0.071). We a priori regarded tree nodes with BSP values 75% or greater and BPP values over 0.95 as sufficiently resolved (*Felsenstein, 2004*; *Huelsenbeck & Hillis, 1993*). BSP values between 75% and 50% (BPP between 0.95 and 0.90) were regarded as tendencies and below 50% (BPP below 0.90) were considered to be not well-supported.

Congruence between nuclear and matrilineal genealogy

We tested if the mitochondrial genealogy of *Solovyeva et al. (2014)* was compatible with our nuDNA phylogeny to eliminate the possibility of mito-nuclear discordance and an introgressed mitogenome. ML trees with unconstrained and alternative constrained topologies were generated for the mitochondrial and nuclear datasets by using Treefinder v.March 2011. Treefinder was also used to calculate site-wise log-likelihoods and to perform the approximately unbiased tree-selection test (AU; *Shimodaira, 2002*).

Significant discordance would have precluded a total evidence approach that evaluated together the mtDNA and nuDNA datasets because we wanted to differentiate between the initial cladogenic event(s) and the timing of interspecific hybridization(s), if present.

Divergence time estimates

The mtDNA dataset of *Solovyeva et al. (2014)* and our nuDNA concatenation were used to define divergence times in BEAST v1.8.0 (*Drummond et al., 2012*). Site and clock models were set as in the species-tree reconstruction. Analyses were run for 100 million of generations and the Yule model was set as the tree prior. Because no reliable paleontological data have been reported for *Phrynocephalus*, we used ten fossils from non-agamid outgroup taxa and outgroup Agamidae as calibration points (see Table S5; Fig. S1).

Area delimitation and biogeographic reconstruction

We used the ML of Lagrange (*Ree et al., 2005*; *Ree & Smith, 2008*) to reconstruct the biogeographic history of *Phrynocephalus*. Transitions between discrete states (ranges) along tree branches were modeled as a function of time, thus enabling ML estimation of the ancestral states at cladogenic events. Lagrange found the most likely ancestral areas at a node, the split of the areas in the two descendant lineages, and calculated the probabilities of these most likely areas at each node (*Ree & Smith, 2008*). We defined seven regions for the analyses: Kazakhstan, North Caspian and Ciscaucasian deserts (KZ), Central Asia (CA), Minor Asia and Transcaucasia (MI), Tibet (TI), Turan (TU), Middle East (ME), and Near East and Arabia (AR) (for details on biogeographic regions definition and references see Supplemental Information 3). The maximum number of regions included in one area was limited to two. We set two periods of time: before 10 Ma and after 10 Ma. This date echoed the considerable uplifting of the Pamir, Tianshan, and Karakoram mountains. (*Abdrakhmatov et al., 1996*). The matrices of the modern distribution areas were given in Table S6.

We reconstructed ancestral substrate niche evolution in *Phrynocephalus* under the MP criterion using MPRsets command in PAUP* v4.0b10 (*Swofford, 2002*) based on nuDNA topology with outgroup taxa included or excluded from the analysis. Polytomies in the nuDNA-based tree were resolved in accordance with the mtDNA topology. To account for topological uncertainty, the analysis was repeated based on a tree sample (180) from the posterior distribution produced by BEAST. Substrate niche was coded using six character states: (1) loose sand dunes; (2) fixed sands mixed with clay or gravel; (3) gravel and stone deserts; (4) clay soils and salines; (5) clay soils mixed with gravel; and (6) large rocks and cliffs. Transitions between states were formalized using step-matrix (Table S7).

To examine the evolution of body size in Agaminae, we used weighted squared-change parsimony (*Maddison, 1991*) as implemented in Mesquite v3.31 (*Maddison & Maddison, 2017*). We tested maximum SVL of taxa reported in literature or based on examination of voucher specimens. Maximum SVLs for each taxon were provided in Table S6.

Table 1 Uncorrected *p*-distances for concatenated sequences of nuDNA (above diagonal) and mtDNA genes (below diagonal) (%) for species groups of *Phrynocepahlu*s (1–11).

#	Group	1	2	3	4	5	6	7	8	9	10	11
1	*arabicus–maculatus*	**11.33/0.70**	2.70	3.00	3.00	3.00	2.10	3.50	2.80	3.14	2.99	3.70
2	*interscapularis*	17.71	**11.45/1.57**	3.40	3.60	3.60	2.50	3.60	3.40	3.40	3.39	3.81
3	*scutellatus*	17.96	18.79	–	3.77	3.67	2.80	3.94	3.87	3.63	3.56	3.99
4	*ocellatus*	17.08	17.24	18.54	**7.09/1.00**	1.52	2.50	1.57	2.90	1.73	1.56	2.00
5	*strauchi*	16.45	16.28	18.40	11.92	–	2.40	1.60	2.82	1.57	1.53	2.00
6	*mystaceus*	17.50	17.90	18.73	14.65	13.77	**7.36/0.4**	2.40	2.46	2.37	2.05	2.60
7	*helioscopus*	18.08	17.68	18.99	14.81	14.14	15.64	**11.09/1.14**	2.92	1.77	1.67	2.07
8	*Oreosaura*	16.47	16.08	18.09	14.26	13.59	15.04	14.80	**7.93/0.75**	2.85	2.50	3.16
9	*axillaris*	16.91	16.79	18.24	14.53	12.72	13.98	13.47	13.52	**2.18/–**	1.08	1.75
10	*versicolor*	16.89	16.89	18.12	14.65	13.21	15.78	15.03	13.65	13.64	**6.95/0.31**	0.60
11	*guttatus*	16.92	17.01	18.27	14.40	13.10	15.16	14.91	13.69	13.48	9.28	**5.84/0.58**

Note:
Values on the diagonal correspond to average uncorrected ingroup *p*-distances for mtDNA\nuDNA genes (%), respectively.

RESULTS

Taxon sampling, data collection, and sequence characteristics

The complete, aligned matrix contained 38 samples of *Phrynocephalus* for mtDNA and 39 samples for nuDNA, representing 33 of the ca. 40 currently recognized species (*Barabanov & Ananjeva, 2007*; *Uetz & Hošek, 2016*). The concatenated aligned mtDNA dataset encompassed 2,703 bp and the nuDNA dataset 1,488 bp. Information on the length of the fragments and variability were given in Table S3. Uncorrected mtDNA genetic distances within *Phrynocephalus* were given in Table 1 (below diagonal).

Phylogenetic inference from mtDNA

Analyses of the mtDNA data resulted in the majority of nodes receiving high BSP and BPP support. Topological patterns were in general congruent across analyses and the results of *Solovyeva et al. (2014)*. The ML tree is shown in Fig. 2. The result appeared to be insensitive to exclusion/inclusion of distant non-agamid and non-agamine outgroups (see Figs. S2 and S3).

Phrynocephalus was unambiguously monophyletic in all analyses (Fig. 2). Several nodes in the mitochondrial tree appeared insufficiently resolved. Nevertheless all species of *Phrynocephalus* were consistently assigned to one of the ten strongly supported matrilines (for their distribution see Fig. S4):

1. Subgenus *Microphynocephalus*, joining the small-sized, sand-dwelling *Phrynocephalus* from Middle Asia and the Middle East (Fig. 2; lineage A).
2. Subgenus *Phrynosaurus* represented by *Phrynosaurus scutellatus* from Iranian Plateau (Fig. 2, lineage B).
3. Near and Middle East *Phrynocephalus*: *Phrynocephalus arabicus* Anderson, 1894 and *Phrynocephalus maculatus* Anderson, 1872 (Fig. 2; lineage C), with the latter species being paraphyletic with respect to the former.
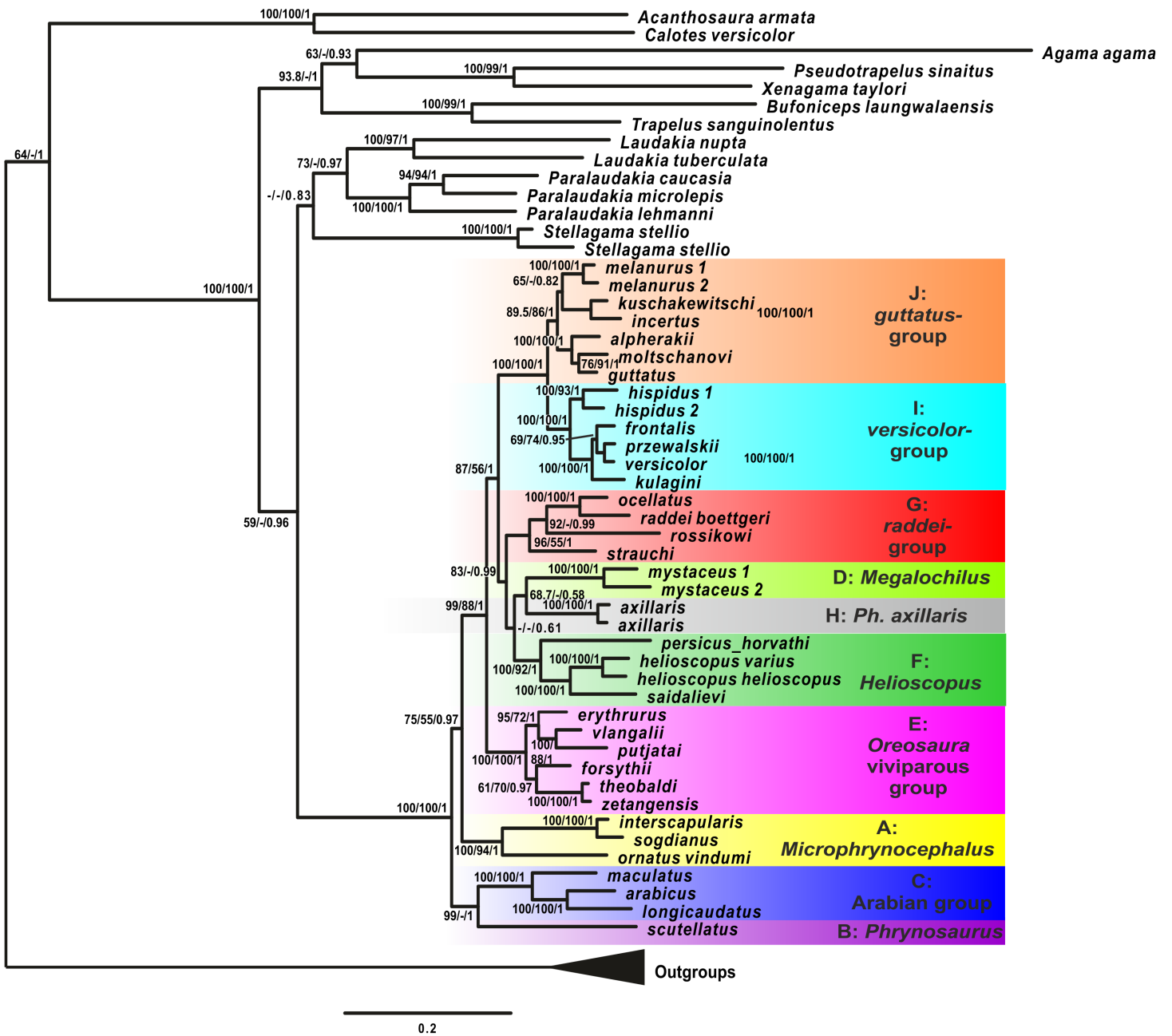
Figure 2 Mitochondrial genealogy of the genus *Phrynocephalus* on the base of 2,703 bp (partial *COI, Cytb, ND2, ND4* sequences). Node support values are given for ML BSP/MP BSP/BI BPP, respectively. Color marking of species groups corresponds to Fig. 3 and Fig. S4.

Full-size ⬚ DOI: 10.7717/peerj.4543/fig-2

4. Subgenus *Megalochilus Eichwald, 1831*, including the large-sized, sand-dwelling *Phrynocephalus mystaceus* (*Pallas, 1776*) from Middle Asia (Fig. 2, lineage D).

5. Subgenus *Oreosaura* joining viviparous Tibetan species (Fig. 2, lineage E).

6. Middle Asian sun-watchers encompassing *Phrynocephalus helioscopus* and allied taxa (Fig. 2, lineage F; *helioscopus*-group).

7. Southern Middle Asian (Turan) *Phrynocephalus raddei* (*Boettger, 1888*), *Phrynocephalus ocellatus*, *P. rossikowi*, and *Phrynocephalus strauchi* Nikolsky, 1899 (Fig. 2, lineage G; *raddei*-group). *P. rossikowi* was omitted in the earlier mtDNA study of *Solovyeva et al. (2014)*; our data strongly support its placement within the *P. raddei* species group.

8. Tibetan oviparous *Phrynocephalus axillaris* Blanford, 1875 (Fig. 2, lineage H).

9. *Phrynocephalus versicolor* species complex, inhabiting northern plains of Central Asia (Fig. 2, lineage I; *versicolor*-group). The *versicolor*-group had two sublineages: *Phrynocephalus hispidus* Bedriaga, 1909 from Mongolian Dzungaria and *Phrynocephalus* sp. 1 from Gansu; and *Phrynocephalus przewalskii* Strauch, 1876 + *Phrynocephalus frontalis* Strauch, 1876 + *P. versicolor* from central China and Mongolia joined with *Phrynocephalus kulagini* Bedriaga, 1909 from Tuva Republic (Russia).

10. *Phrynocephalus guttatus* species complex, widespread in plains of Kazakhstan and northern Caspian region (Fig. 2, lineage J; *guttatus*-group). Within the *guttatus*-group, *P. guttatus*, *Phrynocephalus alpherakii* Bedriaga, 1905 and *Phrynocephalus moltschanovi* Nikolsky, 1913 clustered together.

Phylogenetic inference from nuDNA and mito-nuclear discordance

Maximum likelihood, MP, and BI analyses of the concatenated nuclear DNA dataset resulted in highly congruent trees (Fig. 3). Exclusion of non-agamid taxa did not change the topology significantly (Fig. S5). Phylogenetic trees resulted from separate analyses of individual genes were shown in Figs. S6–S9; values of AU-tests for nuDNA genes compatibility were given in Table S8. The topology of the *BEAST species-tree for *Phrynocephalus* and the levels of nodal support (Fig. 4) coincided with the concatenated nuDNA dataset tree (Fig. 3) and were in good correspondence with the topologies from three of the four nuDNA genes (*NKTR*, *RAG-1*, and *AKAP9*).

Monophyly of *Phrynocephalus* received high support as did several species-groups: *Microphrynocephalus* (Fig. 3, lineage A: 99/100/1), Arabian species-group (Fig. 3, lineage C: 100/100/1), *Megalochilus* (Fig. 3, lineage D: 100/100/1), *Oreosaura* (Fig. 3, lineage E: 100/100/1), and *P. raddei* species-group (Fig. 3, lineage G: 95/84/1). The *P. heliosopus*-group obtained low support (Fig. 3, lineage F:–/–/0.89), but high support in the species-tree (Fig. S4). Monophyly of the clade containing the *P. guttatus*- and *P. versicolor*-groups was highly supported (Fig. 3, lineages I, J: 100/99/1), but interrelationships within this clade remained unresolved. The *P. versicolor*-group was paraphyletic with respect to the *P. guttatus*-group, though with some support only from ELW (Fig. 3: 90/–/–).

The nuDNA phylogeny of *Phrynocephalus* conflicted significantly ($p < 0.05$; AU) from the matrilineal genealogy. The nuDNA topology depicted three main clades (Fig. 3): (1) *Microphrynocephalus*, *P. scutellatus*, Arabian species-group and *Megalochilus* (clades A–D; 99/96/1); (2) *Oreosaura* (clade E; 100/100/1); and (3) all other *Phrynocephalus* (clades F–J; 100/99/1). Most notably, the placements of *Megalochilus* and *Oreosaura* differed in important ways. Matrilineally, *Oreosaura* and *Megalochilus* aligned with
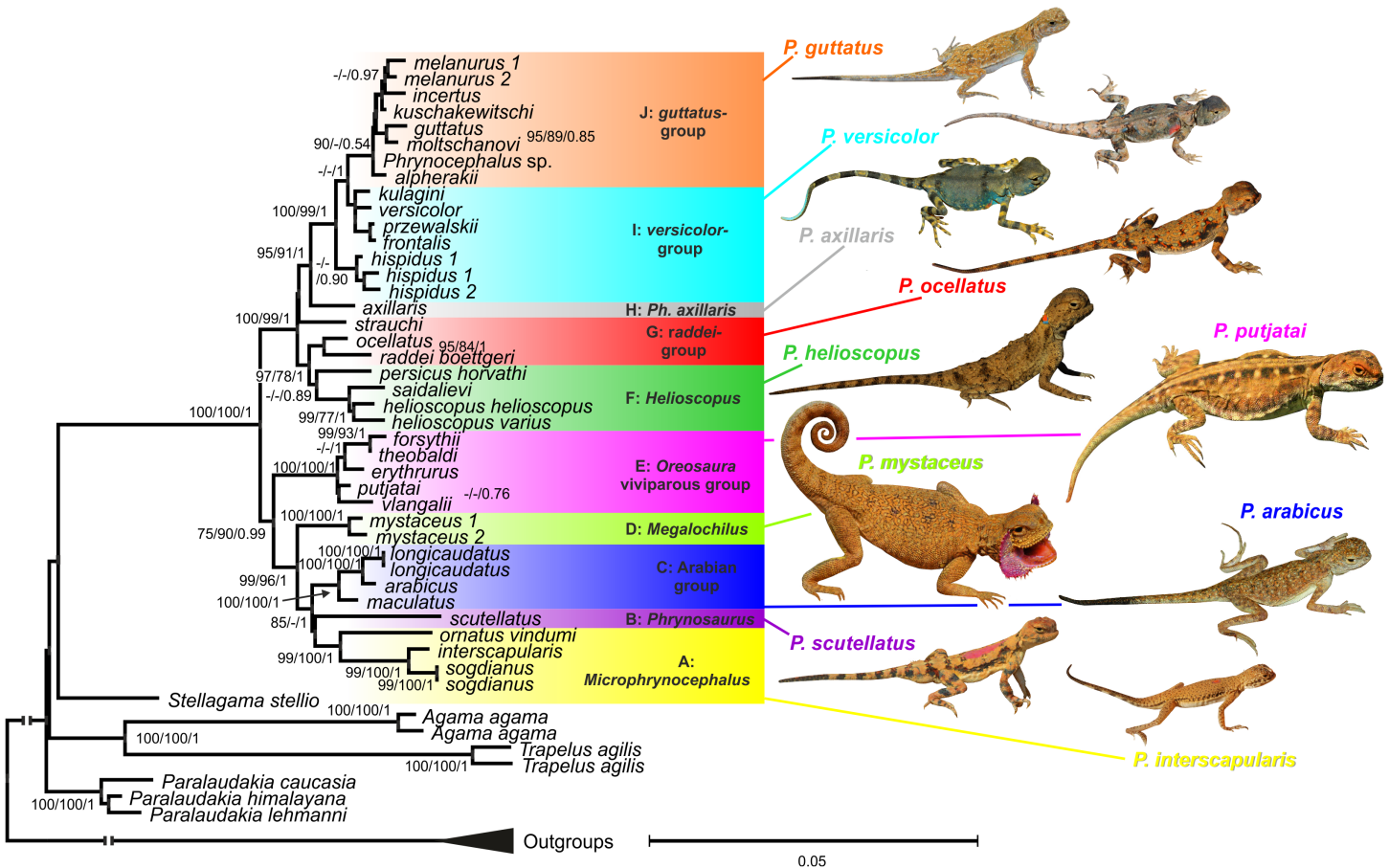
Figure 3 Phylogenetic ML tree reconstructed from concatenated alignment of the nuclear genes *RAG-1, BDNF, AKAP9* and *NKTR.* Numbers on tree nodes indicate bootstrap values (BS) and posterior probabilities for ML BSP/MP BSP/BI BPP, respectively. Color marking of species groups corresponds to mitochondrial lineages; see Fig. 2 and Fig. S4. Thumbnails show representative species of each *Phrynocephalus* species group (to scale; note large size of *P. mystaceus*). Photographs by E. A. Dunayev and R. A. Nazarov. Full-size 🖼 DOI: 10.7717/peerj.4543/fig-3

Middle and Central Asian "core *Phrynocephalus*" with strong support (99/88/1.0). In contrast, the nuDNA biparental phylogeny united *Megalochilus* with Arabian and Iranian species (75/90/0.99), including the *P. arabicus*-group, *P. scutellatus* and *Microphrynocephalus* with *Oreosaura* forming a sister-group to clades A–D. Other notable conflicts also occurred. The nuclear phylogeny did not depict a shared heritage for *P. scutellatus* and the Arabian species-group (Fig. 3), as did the mtDNA genealogy, but rather *P. scutellatus* (clade B) was the sister-lineage of *Microphrynocephalus* (Fig. 2). The phylogenetic position of *P. strauchi* was contentious; analyses of the nuDNA dataset did not group it with the mtDNA *raddei*-group. Similarly, the phylogeny placed *P. axillaris* as a sister-lineage of the *P. guttatus–versicolor*-group (Figs. 3 and 4; Fig. S5; 95/91/1), but its matrilineal relationships were unresolved (Fig. 2).

We performed additional AU tree-selection test to test for significant differences between matrilineal genealogy and the nuclear phylogeny, including whether one or both datasets rejected alternative placements of particular clades. The test evaluated the conflicting positions of *P. mystaceus*, *P. strauchi*, *P. scutellatus*, *Oreosaura*, the basal
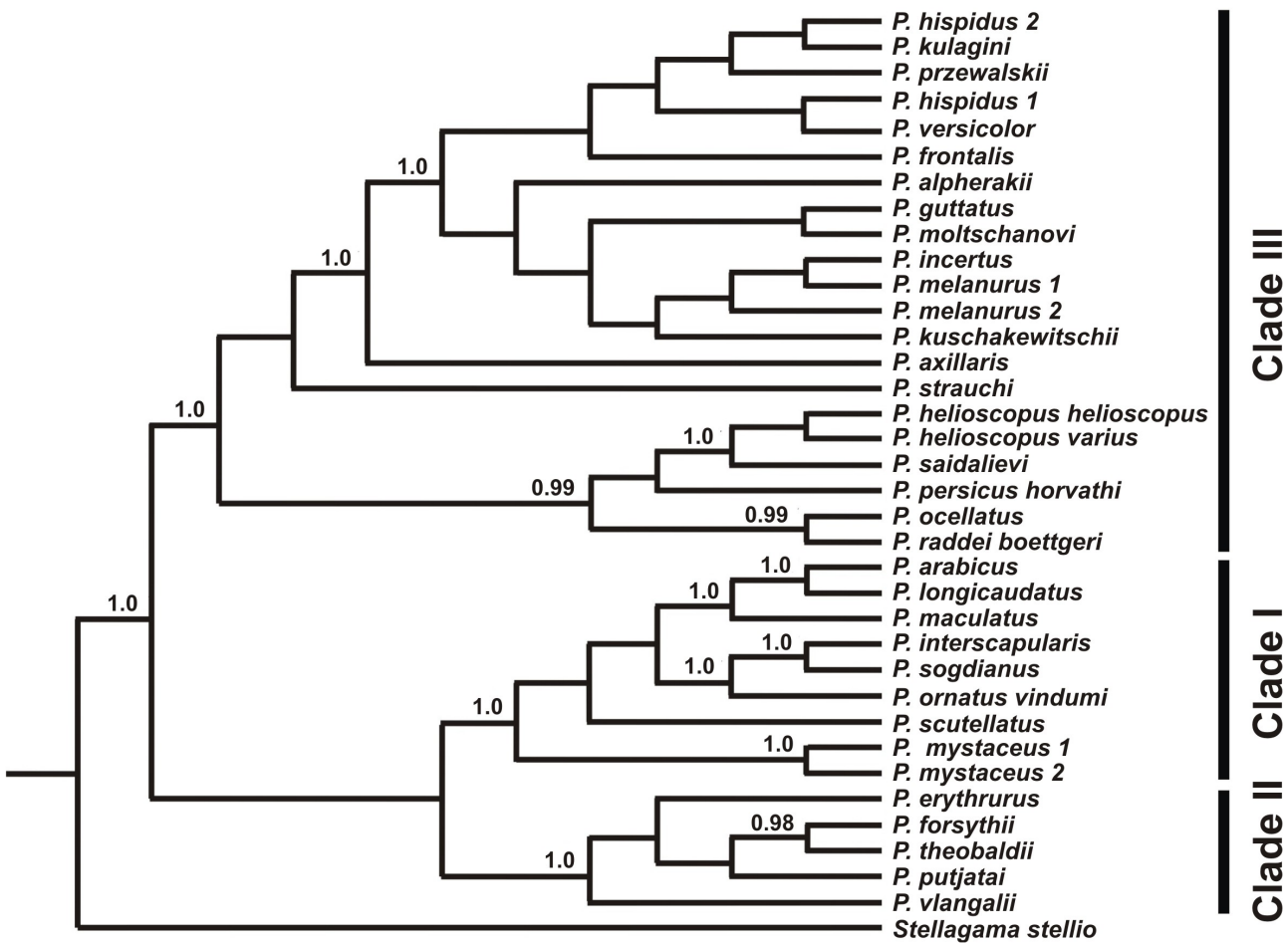
Figure 4 Species tree reconstructed by *BEAST analysis with the nuclear genes *RAG-1*, *BDNF*, *AKAP9*, and *NKTR*. Bayesian posterior probabilities (BI BPP) values are given only for strongly supported nodes. For Clades I–III definitions see "Discussion."

Full-size ◩ DOI: 10.7717/peerj.4543/fig-4

position of Arabian species and Arabian species + *Microphrynocephalus*. The matrilineal genealogy was forced to the nuclear dataset and vice versa. AU indexes for the basal position of Arabian species or Arabian species + *P. scutellatus* in the matrilineal genealogy were not statistically rejected by nuclear markers ($p = 0.217$, $p = 0.277$, respectively). The alternative nuclear hypotheses for the clades A–E and D–H were not rejected by mitochondrial data. The matrilineal position of *P. mystaceus* within the lineage (*Helioscopus* + *P. axillaris* + *P. mystaceus*) was rejected by nuclear markers ($p = 0.000$), and vice versa mitochondrial markers rejected the nuDNA resolution of *P. mystaceus* + Arabian species + *Microphrynocephalus* + *P. scutellatus* ($p = 0.000$). The AU test for *P. strauchi* occurring within the *raddei*-lineage was not rejected statistically by nuclear data ($p = 0.752$) and the mitochondrial data did not reject the nuDNA resolution of *P. strauchi* + *helioscopus*-group ($p = 0.857$). Existence of the matriline *Oreosaura* + "*guttatus*" + "*versicolor*" was rejected according to nuclear data ($p = 0.000$) and vice versa the mitochondrial dataset rejected position of *Oreosaura* within A–E ($p = 0.000$). Finally, we tested topologies of trees based on each nuclear marker against final topology. The *BDNF*

dataset rejected the topology. In contrast, original *RAG-1* topology was rejected. *p*-Values of the AU-tests of alternative topologies were summarized in Table S9.

Divergence times and rates of change

Chronograms from mtDNA and nuDNA data were presented in Figs. S10 and S11, respectively. Timing of the internal nodes was summarized in detail in Table S10. Estimated node-ages and the 95% highest posterior density (95% HPD) for the main nodes were detailed in Table S10. The mtDNA dataset provided older estimates of ages as compared to nuDNA. All analyses proposed that the ancestor of *Phrynocephalus* originated between the end of Oligocene and beginning of the Miocene (mtDNA: 33.2 Ma (26.4–39.7); nuDNA: 26.9 Ma (22.6–31.7)) and the basal radiation dated to the middle Miocene (mtDNA: 19.3 Ma (14.9–23.5); nuDNA 14.8 Ma (12.0–17.5)).

Lineage-through-time (LTT) plots gave a graphical representation of lineage-accumulation (Fig. S12). The mtDNA (Fig. S12A) and nuDNA (Fig. S12B) plots had similar shapes that were best described as being anti-sigmoidal characterized by three periods of constant rate. The first rate constant was separated from the second by a plateau and occurred before 14 Ma for mtDNA and before 11 Ma for nuDNA and the second plateau occurred after these dates. The third period started after 5 Ma, followed by a slight rate-shift in both plots.

Ancestral area, substrate niche, and body size evolution modeling

The ancestral areas and biogeographic processes (vicariance, dispersal, and colonization routes) reconstructed from nuDNA data were shown in Fig. 5. The most likely biogeographic scenario suggested that the Middle East plus the Turan area (ME-TU) was the most probable ancestral area for *Phrynocephalus*, thus supporting the hypothesis of a southern origin. Paleogeography of central Eurasia in Miocene–Pliocene was shown in Fig. 6.

Results of habitat evolution modelling for *Phrynocephalus* were given in Fig. 7. All simulations of the possible evolution of substrate niches in *Phrynocephalus* suggested that the most likely substrate type for the ancestor consisted of soft substrate, i.e., loose sands with non-differentiated proluvial sediments, such as clay or gravel.

Results of ancestral state reconstructions of maximum SVL evolution for each taxon were shown in Fig. 8. Accordingly, the common ancestor of *Phrynocephalus* was likely significantly smaller (size category 87–97 mm) than its sister taxa *Laudakia*, *Stellagama*, and *Paralaudakia* (ancestral size category 147–157 mm). Most species of *Phrynocephalus* have been found to be smaller than their common ancestor (size categories 47–77 mm); however, several lineages of *Phrynocephalus* have subsequently increased their body size (*P. maculatus*: 87–97 mm; *P. mystaceus*: 77–127 mm), while further miniaturization was suggested for the *Phrynocephalus interscapularis*-group (37–47 mm).

DISCUSSION

Phylogenetic relationships of *Phrynocephalus*

Supplemental Information 1 provides a brief review on history of phylogenetic studies of the genus *Phrynocephalus*.

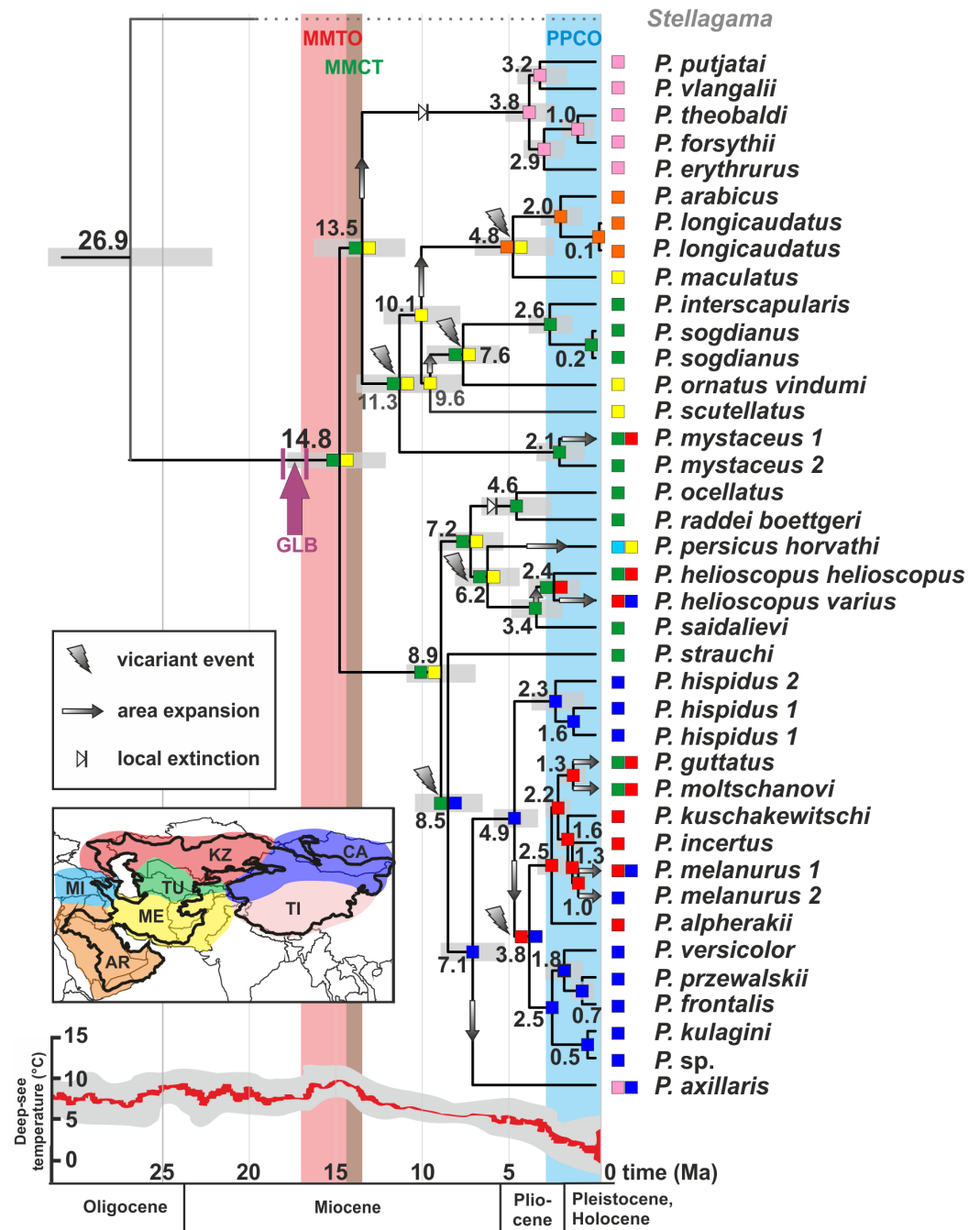**Figure 5 Differentiation of _Phrynocephalus_: BEAST chronogram on the base of nuDNA dataset with results of ancestral area modeling in Lagrange.** GLB, "_Gomphotherium_-landbridge"; MMCT, middle Miocene thermal optimum; MMCT, middle Miocene climatic transition; PPCO, Pliocene–Pleistocene climate oscillations; AR, near East and Arabia, MI, Asia Minor and Transcaucasia; KZ, Kazakhstan, North Caspian and Ciscaucasian deserts; CA, Central Asia; TU, Turan; TI, Tibet; ME, Middle East. For biogeographic areas definitions see Supplemental Information 2 and Table S10. For paleogeographic reconstruction see Fig. 6. Node values correspond to estimated divergence times (in Ma). Icons illustrate vicariant events, area expansion and local extinctions, respectively. Black line on the inset shows modern range of _Phrynocephalus_. Red line corresponds to temperature change during the Cenozoic; climatogram from _Zachos et al. (2001)_. Full-size ⬚ DOI: 10.7717/peerj.4543/fig-5
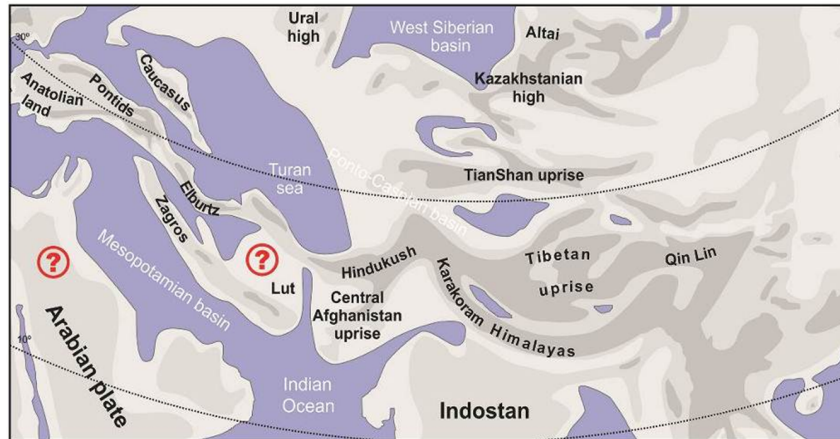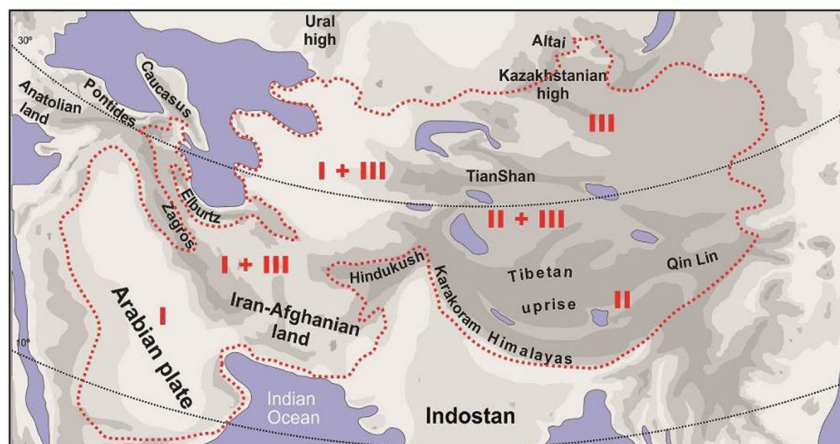
A. Miocene 20-19 Ma

B. Miocene 15-13 Ma

C. Pliocene 3.4-1.8 Ma

Figure 6 Paleogeography of Paratethys basin in late Cenozoic and the hypothetical scenario for *Phrynocephalus*. Paleogeographic reconstructions are based on *Rögl (1999)*; *Popov et al. (2004)*; *Popov et al. (2009)* for early (A) and middle (B) Miocene and Pliocene (C). Question marks denote possible areas of distribution of the common ancestor of Phrynocephalus. GLB—"*Gomphotherium*-landbridge" between Arabian plate and Asian mainland (18–17 Ma). Red dotted line—possible range of *Phrynocephalus*; red arrows—possible dispersal routes; Latin numbers correspond to hypothetical distribution of main Phrynocephalus Clades I–III (see Discussion).

Full-size 🖼 DOI: 10.7717/peerj.4543/fig-6

Phylogenetic placement of *Phrynocephalus*. Our results are in accordance with previous studies on the higher phylogenetic relationships within the subfamily Agaminae (*Macey et al., 2000*; *Guo & Wang, 2007*; *Melville et al., 2009*) (Figs. 2 and 3). Sand-dwelling *Bufoniceps laungwalaensis* (*Sharma, 1978*) from the Thar Desert of India, which was originally described as a species of *Phrynocephalus* (*Sharma, 1978*), is the sister-lineage of the Middle Eastern–Middle Asian genus *Trapelus*; this corresponds with results of *Macey et al. (2006)* and *Melville et al. (2009)*. The clade (*Phrynocephalus* + *Laudakia* s.l.) is poorly resolved; the old age of this radiation, which we estimate as early to mid-Oligocene (Figs. S10 and S11), likely complicates phylogenetic resolution. Future genome-scale studies are likely to recover these relationships. Regardless, the monophyly of *Phrynocephalus* (excluding *B. laungwalaensis*) is unambiguous in all analyses.

Phylogenetic relationships within *Phrynocephalus*. Analyses of nuclear gene exons (Fig. 3) resolve the phylogenetic relationships for most of the species-groups revealed by the matrilineal genealogy (Fig. 2), including the following: *P. interscapularis*-group (subgenus *Microphrynocephalus*; lineage A on mtDNA-genealogy), subgenus *Oreosaura* (lineage E), *P. guttatus*- and *P. versicolor*-groups (lineages J and I, respectively), *P. mystaceus* (subgenus *Megalochilus*; lineage D), *P. helioscopus* (lineage F), and *P. arabicus*–*P. maculatus* (lineage C). The *P. guttatus*- and *P. versicolor*-matrilines are sister-groups, although concatenated analyses of nuDNA data nest the former within the latter (Fig. 3) and the species-tree suggests sister-group relationships (Fig. 4). These are the youngest associations within *Phrynocephalus*. MtDNA analyses resolve close relationships between the *P. helioscopus*-group and *P. axillaris*, but analyses of nuDNA data resolve *P. helioscopus*-lineage + *P. ocellatus*-lineage with strong support and place *P. axillaris* as the sister clade to the *P. guttatus* + *P. versicolor* lineages.

Overall, the nuDNA phylogenetic trees are generally better resolved and show higher nodal support values than the mtDNA trees. The nuDNA phylogeny also shows higher congruence with traditional systematics of the genus. Owing to biparental inheritance, we prefer the nuDNA topology as the phylogeny of the genus *Phrynocephalus* (Fig. 3), which coincides well with the species-tree (Fig. 4). Further, the matrilineal genealogy appears to resolve the introgression of mitogenomes via interspecific hybridization (below). In general, *Phrynocephalus* has three main clades, but the relationships among them are not well-supported.

Clade I (Fig. 4) contains the *P. interscapularis*-group (subgenus *Microphrynocephalus*), *P. arabicus*–*P. maculatus*-group, *P. scutellatus* and *P. mystaceus* (subgenus *Megalochilus*). The phylogenetic relationships between these four groups are essentially unresolved.
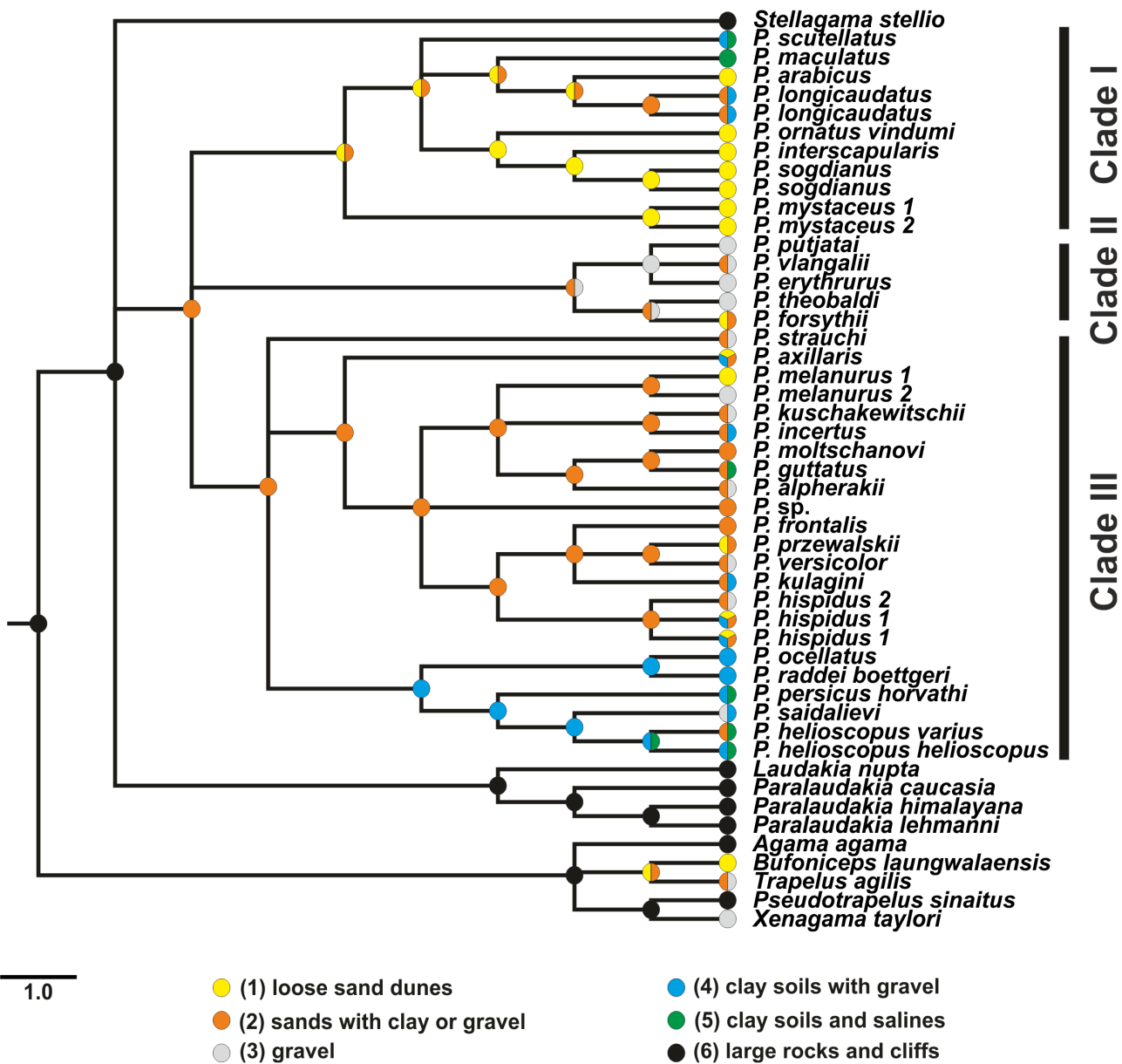
Figure 7 Evolution of habitat preference in the Agaminae including the genus *Phrynocephalus*. See "Materials and Methods" and Table S5 for habitat data and Table S6 for step-matrix showing transition between substrate niche states. Agaminae outgroups, except for *Xenagama*, *Trapelus*, and *Bufoniceps*, inhabit large rocks and cliffs. Two lineages within the subfamily independently adapted to sandy habitats: the common ancestor of *Bufoniceps* and *Trapelus* and the ancestor of *Phrynocephalus*. Main groups within *Phrynocephalus* evolved adaptations to life on large loose sand dunes (*P. arabicus*, *P. mystaceus* and *Microphrynocephalus*), stony and gravel highland deserts (subgenus *Oreosaura*), and on clay substrates with gravel (*P. helioscopus–P. raddei* group). Full-size ◳ DOI: 10.7717/peerj.4543/fig-7

This groups includes oviparous species inhabiting Arabia, Near to Middle East, and Middle Asia. Many of them associate with sand dunes. Monophyly of the *P. arabicus–maculatus* group and *Microphrynocephalus* (*P. interscapularis–Phrynocephalus ornatus* Boulenger, 1887-group) has strong support.
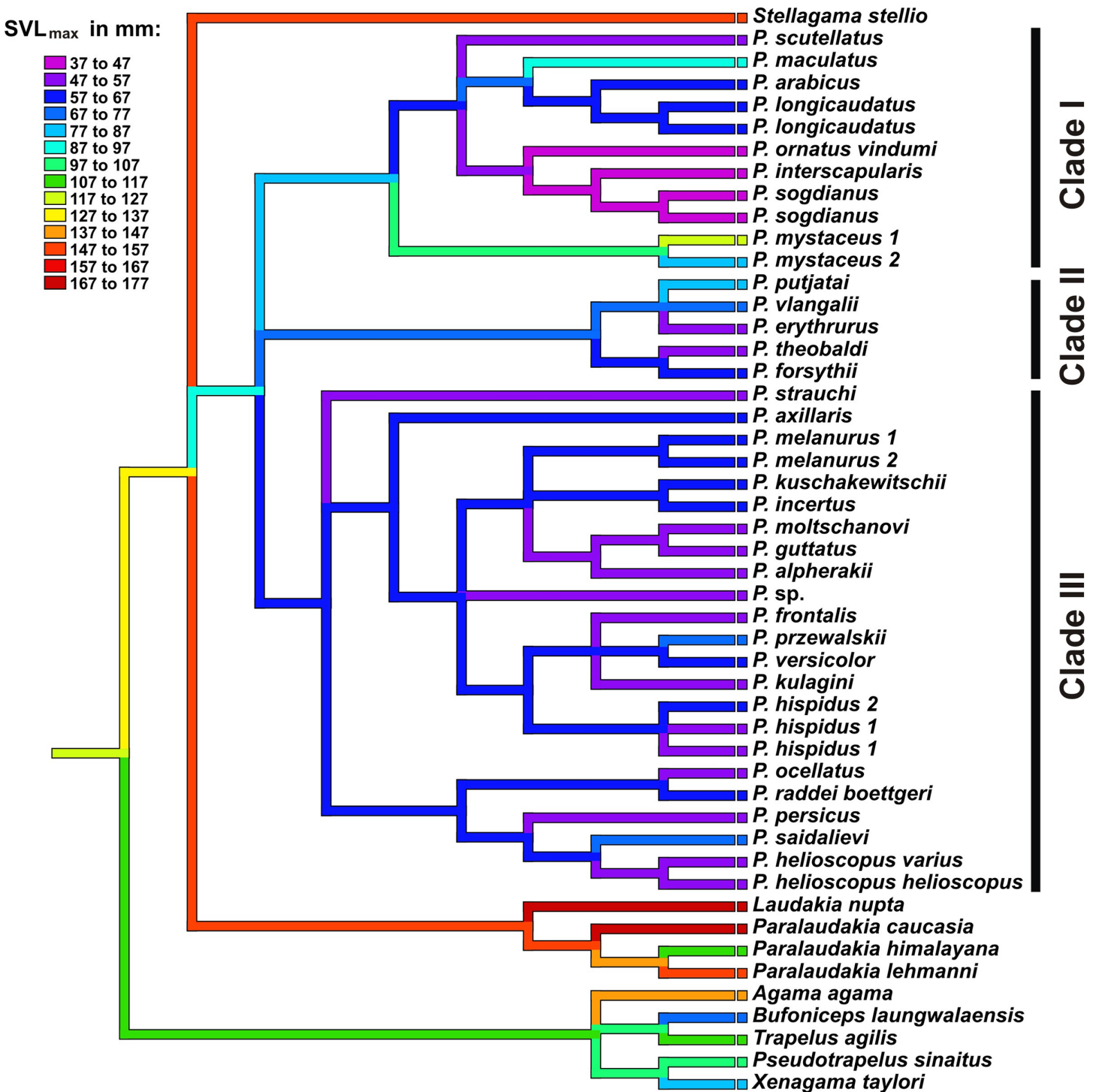
Figure 8 Body size evolution among Agaminae including genus *Phrynocephalus*. See Table S5 for maximum SVL data. Color of branches corresponds to SVL$_{max}$ (see legend). Rock-dwelling *Laudakia* s.l. are characterized by larger body size, while the common ancestor of *Phrynocephalus* was likely smaller than other Agaminae; sand-dwelling *Microphrynocephalus* (*P. ornatus*–*P. interscapularis* group) and *Megalochilus* (*P. mystaceus* group) represent the most miniaturized and the largest lineages within the genus, respectively.

Full-size 🖼 DOI: 10.7717/peerj.4543/fig-8

Clade II (Fig. 4) includes viviparous species inhabiting high elevations of the QTP (subgenus *Oreosaura*). Phylogenetic relationships within this group remain unresolved with the exception of a sister-species relationship between *Phrynocephalus theobaldi* Blyth, 1863 and *Phrynocephalus forsythii* Anderson, 1872. In the concatenated analysis of nuDNA exons (Fig. 3), monophyly of the group that includes clade I and clade II receives strong support (75/90/0.99), although this node does not receive high support in the species-tree analysis (Fig. 4).

Clade III (Fig. 4), the "core" *Phrynocephalus*, contains all remaining taxa of the genus and consists of oviparous lowland species inhabiting arid areas of Central and Middle Asia and the Middle East. It includes two strongly supported groups: *P. helioscopus–P. raddei* and *P. guttatus–P. versicolor*. Monophyly of the *P. helioscopus* species complex and the *P. ocellatus–P. raddei*-group receives strong support. The phylogenetic position of *P. strauchi* remains unresolved, while *P. axillaris* appears as the sister-taxon of the *P. guttatus–P. versicolor*-group, which coincides with morphology; *P. axillaris* and members of the *P. guttatus–P. versicolor* species complexes share a number of morphological similarities, including having bright axillary spots possibly used in signaling communication (Fig. 3).

Our phylogeny has better resolution and wider taxon sampling than previously published mtDNA-based genealogies (*Pang et al., 2003*; *Guo & Wang, 2007*; *Melville et al., 2009*; *Solovyeva et al., 2014*) and the nuDNA-based phylogeny (1,200 bp fragment of *RAG-1*) of *Melville et al. (2009)*. Our tree also differs from the morphological phylogeny of *Arnold (1999)*, in which the Tibetan viviparous *Oreosaura* appear to be deeply nested within the core clade of *Phrynocephalus* and nests with the *P. helioscopus*-group, while *P. mystaceus*, *P. arabicus*, *Phrynocephalus longicaudatus Haas, 1957* (as *P. maculatus*) and *Microphrynocephalus* occupy the basal position in the *Phrynocephalus* radiation. The potential explanation of these differences may be connected with habitat preferences; adaptation to types of substrate may drive convergent changes and morphology. Both Tibetan viviparous *Oreosaura* and *P. helioscopus*-group members occur mostly on solid (rocky or clay) substrates and are superficially similar in external morphology, sharing robust body habitus, shortened tail, and other features. At the same time, sand-dwelling *Microphrynocephalus*, *P. mystaceus* and *P. arabicus* and *Bufoniceps* share such characters as presence of enlarged scale fringes on toes, enlarged or keeled scales on throat, eyelids or jaws, flattened body and tail, which are considered to be adaptive for life on large wind-blown sand dunes. *Arnold (1999)* rooted his tree with *Trapelus* and *Bufoniceps*. However, convergent similarity between send-dwelling *Phrynocephalus* and *Bufoniceps* potentially could lead to the basal position of *P. mystaceus*.

Mito-nuclear discordance due to ancient hybridization. The main difference between mt- and nuDNA trees is the positions of *P. mystaceus*: the nuDNA-based topology strongly suggests that *P. mystaceus* as a sister-group with respect to the Middle-Eastern *P. interscapularis*-group (*Microphrynocephalus*), *P. scutellatus* and the Arabian *P. arabicus–P. maculatus*-group (Fig. 3). In contrast, the mtDNA genealogy unambiguously places *P. mystaceus* within core *Phrynocephalus* with *P. axillaris* being a possible sister-lineage (Fig. 2). The AU tests either rejects or do not provide statistical support for genomic compatibility (except as noted above; Table S8). Mitochondrial and nuclear genetic

markers have yielded many conflicting geographic patterns (reviewed by *Toews & Brelsford, 2012*). Examples of mito-nuclear discordance in reptiles remain limited (*McGuire et al., 2007*; *Zarza et al., 2011*; *Pedall et al., 2010*; *Renoult et al., 2009*; *Leache & Cole, 2007*; *Ng & Glor, 2011*; *Nguyen et al., 2017*), perhaps because the discrepancy is rarely tested. Different mechanisms and rates of evolution for mt- and nuDNA may account for some observed topologic discrepancies. *Fisher-Reid & Wiens (2011)* evaluated 14 vertebrate clades for which both mtDNA and nuDNA data exist and reported that 30–60% of the nodes differed between trees from the two genomes. The results of our AU-tests suggest that topological differences between mtDNA and nuDNA hypotheses can be statistically significant. Thus, our analyses suggest that the combining of data from the two genomes should be avoided or done with caution without first testing for compatibility. Equally important, analyses based on combined datasets may hide biogeographic histories of studied taxa due to gene sorting, genetic recombination and gene flow of nuDNA (*Nguyen et al., 2017*).

Several processes, including incomplete lineage sorting or introgressive hybridization, may best explain mito-nuclear discordance (*Toews & Brelsford, 2012*). The deep divergence between *P. mystaceus* and core *Phrynocephalus*, as well as the unique morphology of this large-sized species differing from any other congener (Fig. 3), renders incomplete lineage sorting an unlikely scenario (*McGuire et al., 2007*). Thus, in case of *P. mystaceus*, an ancient introgression of mitochondrial genome due to interspecific hybridization best explains the discordance. According to mtDNA time-tree (Fig. S10) divergence between mitochondrial genomes of ancestral *P. mystaceus* and *P. axillaris* took place in late Miocene (around 10.4 Ma), whereas the basal differentiation of *Phrynocephalus* is estimated as the middle Miocene (around 14.8 Ma; Fig. S11) according to nuDNA data. Hence, the possible hybridization between *P. mystaceus* and *P. axillaris* ancestors occurred approximately 5 Ma after speciation, and this roughly corresponds to the level of divergence within the present-day *P. guttatus*–*P. versicolor* species complexes. This timing makes interspecific hybridization possible. Further, male-biased dispersal favors mitochondrial genome introgression (*Toews & Brelsford, 2012*) and *Phrynocephalus* appears to have male-mediated gene flow. Discordant breaks in mtDNA and nuDNA markers occur in at least for four species: *Phrynocephalus vlangalii*–*Phrynocephalus putjatai* Bedriaga, 1909-groups (*Noble, Qi & Fu, 2010*; *Qi et al., 2013*), and in the *P. przewalskii*–*P. frontalis*-groups (*Urquhart, Wang & Fu, 2009*). Other lineages may have the same pattern. *P. mystaceus* is the largest species of the genus and it shows adaptations typical of a psammophilous lifestyle including triangular scales forming fringes on toes, ridged subdigital lamellae, distinctly flattened body and tail, and a pair of unique cutaneous flaps at mouth corners with numerous spiny scales along flap edges. Similar spiny scales can occur in mouth corners of miniaturized psammophilous members of the *P. interscapularis*-group and *Phrynocephalus euptilopus* Alcock et Finn, "1896" 1897. These species are similar to *P. mystaceus* and occur in the Middle East and Middle Asia. Thus, our nuDNA phylogenetic hypothesis corresponds with life history, biogeographic, and morphological similarities between *P. mystaceus* and smaller psammophilous taxa of *Phrynocephalus*.

Taxonomic implications

The results of our phylogenetic analyses require some taxonomic changes within *Phrynocephalus*. These include recommendations on genus- and species-level taxonomy.

Generic taxonomy of *Phrynocephalus*. The significant morphological diversity of *Phrynocephalus* has been reflected in their generic taxonomy. First, *Eichwald (1831)* proposed the new name *Megalochilus* for the largest species of the genus, *P. mystaceus*. *Ananjeva (1987)* recognized the genus, but this was not accepted by subsequent researchers (*Zhao & Adler, 1993*; *Dunayev, 1996b*; *Arnold, 1999*). *Sharma (1978)* described *P. laungwalaensis* from Rajasthan (India), but *Arnold (1992)* removed it from *Phrynocephalus* and reassigned it to monotypic *Bufoniceps*, which he treated as a sister-clade of *Phrynocephalus*. Subsequent molecular analyses supported this arrangement (*Macey et al., 2006*; *Melville et al., 2009*). Based on the phylogenetic analysis by *Pang et al. (2003)*, *Barabanov & Ananjeva (2007)* suggested recognizing the Tibetan viviparous species-group as subgenus *Oreosaura*. Because the phylogenetic relationships within oviparous species remained largely unknown, this subgeneric taxonomy was not largely accepted. *Solovyeva et al. (2014)* analyzed four mtDNA gene fragments and the morphological data of *Arnold (1999)* and suggested that small-bodied sand-dwelling *Phrynocephalus*, including the *P. interscapularis*-group and *P. ornatus*, constituted a morphologically and phylogenetically distinct group; they erected new subgenus *Microphrynocephalus* for it. However, our nuDNA-based phylogeny requires reconsideration of this arrangement.

Excluding *B. laungwalaensis*, nuDNA, mtDNA (herein), and morphological (*Arnold, 1999*) analyses indicate monophyly of *Phrynocephalus*. Thus, the splitting of *Phrynocephalus* into several genera is inadvisable. Further molecular studies are necessary to test for monophyly of *Laudakia* s.l. and its relationships with respect to *Phrynocephalus*.

The recognition of subgenera within *Phrynocephalus* is a matter of taste. The genus has three clearly defined clades that may warrant taxonomic recognition. The largest of these clades, or the "core" *Phrynocephalus* (clade III, Fig. 4), encompasses the majority of oviparous species and corresponds to the nominative subgenus *Phrynocephalus* s.s. clade II (Fig. 4) unites viviparous species of the QTP and is well-defined by morphology and life history traits; subgenus *Oreosaura* applies to it. Last, clade I (Fig. 4) joins a number of species from Arabia, Middle East and Middle Asia that have plesiomorphic character states (*Arnold, 1999*, including the *P. arabicus–P. maculatus*-group, *P. interscapularis–P. ornatus*-group, *P. scutellatus* and *P. mystaceus*. The *P. interscapularis–P. ornatus*-group, which was erected as subgenus *Microphrynocephalus* Dunayev, Solovyeva, Poyarkov, 2014 (*Solovyeva et al., 2014*) are miniaturized species adapted to life in aeolian sand habitat and they share a number of morphological synapomorphies (*Arnold, 1999*) and geographic coherence. The older name *Phrynosaurus* Fitzinger, 1843 is available. However, the phylogenetic position of its type species—*P. olivieri* Duméril et Bibron, 1837, which is now considered as a junior synonym of *P. scutellatus* (Olivier)—within the clade remains unclear. Finally, *P. mystaceus*, to which the name *Megalochilus Eichwald, 1831*, is available, forms a sister-group with respect to all other members of clade I. This

species has a unique morphology and evolutionary history, which likely includes an episode of ancient intraspecific hybridization with introgression of its mitochondrial genome from clade III species.

Two alternative taxonomic decisions are possible: recognizing the whole of clade I as *Megalochilus*, or splitting it into a number of smaller taxa, including *Megalochilus*, *Phrynosaurus*, *Microphrynocepahlus*, and an unnamed taxon for the *P. arabicus–P. maculatus* species group. Our analyses lack samples from a number of Middle Eastern species, which likely fall into clade I, including *P. ornatus ornatus*, *Phrynocephalus clarkorum* Anderson et Leviton, 1967, *Phrynocephalus lutensis Kamali & Anderson, 2015*, *Phrynocephalus luteoguttatus* Boulenger, 1887 and, most importantly, large-sized and psammophilous *P. euptilopus*. Accordingly, we suggest that further taxon sampling and additional nuDNA-markers be evaluated before making subgeneric changes in the interest of maintaining taxonomy stability.

Taxonomic differentiation within species complexes. Our results indicate that in many cases the currently adopted taxonomy is incomplete and does not reflect the actual biodiversity within *Phrynocephalus*. We briefly review these cases and provide corresponding taxonomic recommendations.

Lineage A. *Microphrynocephalus*. This group of miniaturized species inhabit wind-blown sands of southern Middle Asia (Turan) and Middle East. Our analyses include *P. interscapularis*, *Phrynocephalus sogdianus Chernov, 1948* and *P. ornatus vindumi* Golubev, 1998 only. Although unsampled, *P. ornatus ornatus*, *P. clarkorum*, *P. luteoguttatus*, *P. lutensis* most likely belong to this group based on morphological characters (*Arnold, 1999*; *Kamali & Anderson, 2015*). *P. sogdianus* was described from southern-most Tajikistan by *Chernov (1948)* as a subspecies of *P. interscapularis* (type locality "vicinity of the Pyandzh [=Panj] village"). Later, *Sokolovsky (1975)* raised it to be a full species. Our locality for *P. sogdianus*, Kurjalakum Sands, occurs approximately 50 km from the type locality and the Vakhsh River Valley separates it from the type locality. Our substantial divergence in mtDNA sequences (uncorrected genetic p-distance = 3.9–4.3% for *COI*) coincides with morphological and distributional differences and favors the recognition of *P. sogdianus* as a full species.

Lineage B. *Phrynocephalus scutellatus*. The phylogenetic position of this small-sized species, which inhabits clay or gravel deserts on the Iranian Plateau, remains unclear within clade I. The recent molecular study of *Rahiamian et al. (2015)* identified at least four highly divergent matrilines in southern and north-eastern Iran. Thus, *P. scutellatus* might consist of a species complex that requires reconsideration.

Lineage C. Arabian group. Our analyses include psammophilous *P. arabicus* s.l., which inhabits aeolian sand dunes from the Arabian Peninsula to westernmost Iran, and *P. maculatus*, which occurs on hard substrates and has two presently recognized subspecies: *P. m. maculatus* (Anderson) from the Iranian Plateau and *P. m. longicaudatus* from the Arabian Peninsula. Our sampling lacks *Phrynocephalus golubewii* Shenbrot et Semenov, 1990 from Turkmenistan and *Phrynocephalus sakoi* Melnikov, Melnikova, Nazarov, Al-Johany & Ananjeva, 2015 from Oman. *Melnikov et al. (2014)* revised *P. arabicus* complex, considered *Phrynocephalus nejdensis Haas, 1957* and *Phrynocephalus*

macropeltis Haas, 1957 as valid species, and described the population of *P. arabicus* s.l. from western Iran as the new species *Phrynocephalus ahvazicus* Melnikov, Melnikova, Nazarov, Rajabizadeh, Al-Johany, Amr & Ananjeva, 2014. However, this taxonomic action was based primarily on small to moderate genetic distances between these forms (*p*-distance 2.7–6.0%) and differences observed in coloration of living animals. Because *Melnikov et al. (2014)* did not include many morphological and meristic characters that serve to diagnose the species, these data must be taken with caution (*Kamali & Anderson, 2015*). Our sample from western Iran corresponds to *P. ahvazicus* of *Melnikov et al. (2014)*. However, we tentatively assign it as *P. arabicus* s.l. pending a further re-assessment of the taxonomy of the *P. arabicus* species complex. Previously, *Solovyeva et al. (2014)* suggested that paraphyly of *P. maculatus* s.l. occurred with respect to *P. arabicus.* Our multilocus nuDNA-based phylogeny agrees with the matrilineal genealogy and indicates that *P. longicaudatus* from the Arabian Peninsula is a sister-taxon of *P. arabicus* (*p*-distance = 8.0% for *COI*). This differs from *P. maculatus* from Iran being reconstructed as a sister-taxon to the clade joining *P. arabicus* and *P. longicaudatus.* Based on the principle of monophyly, as well as genetic and distributional differences, we raise *P. longicaudatus* to full species status as *P. longicaudatus* (*Haas, 1957*) **comb. et stat. nov.**

Lineage D. *Megalochilus*. *P. mystaceus* represents a widespread species-complex that inhabits wind-blown sands and large sand dunes from north-eastern Iran to the Turan region, Middle Asia, and the Caspian Basin. While intraspecific taxonomy within *P. mystaceus* is in a state of flux, we report on two highly divergent lineages within this complex that were firstly revealed by mtDNA sequences (*Solovyeva et al., 2014*; *p*-distance = 6.3–6.5% for *COI*). Nuclear markers also reveal deep divergence between these two lineages, one of which is restricted to East Khorasan Province, Iran (*P. mystaceus* 2) and another occupies the rest of species range in Middle Asia (*P. mystaceus* 1). Thus, the taxonomy of this complex requires further study.

Lineage E. *Oreosaura*. This clade consists of viviparous highland species inhabiting deserts of the QTP and our analyses evaluate *Phrynocephalus erythrurus*, *P. forsythii*, *P. putjatai*, *P. vlangalii*, and *P. theobaldi* within the complex. The phylogenetic relationships among these species remain essentially unresolved. *Pang et al. (2003)*, *Jin, Brown & Liu (2008)*, *Jin, Liu & Brown (2017)*, *Jin & Liu (2010)*, *Noble, Qi & Fu (2010)*, and *Zhang et al. (2010)* assessed their phylogenetic relationships and biogeography.

Lineage F. *P. helioscopus*–*Phrynocephalus persicus*-group. This group, which was until recently considered to be a widespread polytypic species *P. helioscopus* s.l., occurs in the montane deserts from western and northern Iran, Transcaucasia, the Turan Region, and Middle Asia to the Caspian Basin in the west and westernmost China and Mongolia in the east. *P. helioscopus* has a robust, tuberculate morphology and inhabits mostly hard substrates in clay or clay/gravel deserts. Previous phylogenetic analyses of mtDNA (*COI*) and nuDNA (interSINE-PCR) by *Solovyeva et al. (2011)* indicated the presence of two main clades within this complex: *P. helioscopus* complex (Middle Asia and adjacent territories) and *P. persicus* De Filippi, 1863 complex (Iran and Transcaucasia), both of which contained a number of highly divergent lineages. Subsequent analysis of morphological characters resulted in recognizing seven subspecies within *P. helioscopus*

and three within *P. persicus* (*Solovyeva, Dunayev & Poyarkov, 2012*). Our phylogeny does not support monophyly of the *P. helioscopus* + *P. persicus* group (Fig. 2), although the species-tree does (Fig. 4). The *P. helioscopus* complex is a monophyletic unit. Deep divergences in both mtDNA and nuDNA genes occur between *Phrynocephalus saidalievi* Sattorov, 1981 from Ferghana Valley, Uzbekistan, and Tajikistan and *P. h. helioscopus* + *P. h. varius Eichwald, 1831* (*p* = 12.0–12.6% in *COI*). *Eremchenko & Panfilov (1999)* proposed full species status for *P. saidalievi* based on differences in karyotype and our analyses strongly support this arrangement. Based on the principle of monophyly, along with the molecular and morphological analyses of *Solovyeva et al. (2011)*, *Solovyeva, Dunayev & Poyarkov (2012)*, we also recognize *Phrynocephalus meridionalis* Dunayev, Solovyeva, Poyarkov in Solovyeva, 2012 **comb. et stat. nov.** This species is the sister-taxon of *P. saidalievi* and was originally described as a subspecies of *P. helioscopus* from the Surkhandarya Region of southern Tajikistan. The species differs markedly in its mtDNA sequences (*p* = 10.0–10.6% in *COI*), nuclear markers and morphology (*Solovyeva et al., 2011*, *Solovyeva, Dunayev & Poyarkov, 2012*). Future studies can address further taxonomic reassignments within the *P. helioscopus* and *P. persicus* complexes.

Lineage G. *P. raddei–P. ocellatus* group. This group contains a number of species that have comparatively small distributions involving gravel or clay-gravel deserts of Turkmenistan, Uzbekistan, and eastern Tajikistan. Unfortunately, we were unable to obtain nuDNA sequences from our sample of *P. rossikowi* due to poor quality of the DNA from this sample; however, our mtDNA analysis strongly suggests that *P. rossikowi* is a member of this species group, and this is concordant with morphological similarity and ecology of this species, which prefer solid substrates (salines) (*Solovyeva, 2017*). Until recently, with the exception of *P. rossikowi*, two species were recognized: *P. raddei* Boettger, 1888 (subspecies *P. raddei raddei* Boettger, 1888 from Turkmenistan and *P. raddei boettgeri* Bedriaga, 1905 from Uzbekistan) and *Phrynocephalus reticulatus Eichwald, 1831* (subspecies *P. re. reticulatus Eichwald, 1831* from Uzbekistan, *P. re. bannikovi* Darevsky, Rustamov et Shammakov, 1976 from Turkmenistan and *P. re. strauchi* from Ferghana Valley in Uzbekistan and Tajikistan; *Terentjev & Chernov, 1949*; *Wermuth, 1967*, *Bannikov et al., 1977*; *Barabanov & Ananjeva, 2007*). *Barabanov & Ananjeva (2007)* considered *P. boettgeri* a junior synonym of *P. raddei*. *Golubev (1991)* examined the type specimens of *Agama ocellata* Lichtenstein in Eversmann, 1823 and demonstrated that it was the senior synonym of *P. reticulatus Eichwald, 1831*, which he considered as a subjective junior synonym of the former. Subsequently, the name *P. ocellatus* (Lichtenstein in Eversmann, 1823) was widely accepted for over 25 years (*Dunayev, 1996b*, *2008*; *Golubev et al., 1995*; *Manilo, 2000*, *2001*; *Manilo & Golubev, 1993*; *Szczerbak, 1994*; *Solovyeva et al., 2014*). Despite that, *Barabanov & Ananjeva (2007*: 56*)* proposed to protect the name *P. re. reticulatus* and in doing so violated the principle of priority (*ICZN, 1999*). Herein, we follow Golubev (1991) and use the name *P. ocellatus* in order to maintain nomenclatural stability and priority.

Our mtDNA analyses suggest monophyly of the *P. raddei boettgeri–P. ocellatus* group and suggest that *P. strauchi* is their sister-group. Their relationships within *Phrynocephalus*

remain unresolved (Fig. 2). Concatenated (Fig. 3) and species-tree (Fig. 4) analyses of nuclear loci resolve paraphyly within the group. The phylogenetic position of *P. strauchi* is unresolved and *P. raddei boettgeri–P. ocellatus* form a well-supported sister-group relationships with *P. helioscopus–P. persicus* (lineage F). This clearly supports giving full-species status of *P. strauchi* as suggested by *Dunayev (1995)*. Our sampling within this group is incomplete because we lack *P. bannikovi* and *P. raddei raddei* from Turkmenistan. Further studies are required to clarify phylogenetic relationships within this group.

Lineage H. *P. axillaris*. Oviparous *P. axillaris* from sand deserts of Taklimakan and adjacent parts of western China is a highly divergent lineage according to our concatenated (Fig. 3) and species-tree (Fig. 4) analyses of nuDNA-markers. It is the sister-taxon of lineages I–J (*P. guttatus–P. versicolor*-group). These lizards have a slender habitus, share habitat preferences and have bright red to blue axillary spots used in intraspecific communication (Fig. 3). *Zhang et al. (2010)* reported on the phylogeography of this species.

Lineages I–J. *P. guttatus–P. versicolor* group. Analyses of both mtDNA (Fig. 2) and nuDNA (Figs. 3 and 4) datasets suggest monophyly of the group. They are morphologically diverse oviparous species from lowland deserts of northern Middle and Central Asia. While analyses of the mtDNA data indicate reciprocal monophyly of *P. guttatus* and *P. versicolor* lineages, analyses of nuDNA data nest latter within the former. The *P. guttatus*-group (lineage J) inhabits various types of deserts ranging from sand dunes to gravel deserts. They occur in the Middle Asia from Caspian Basin to the westernmost China. *Dunayev (1996a, 2009)* assessed the taxonomy and distribution of lizards in Kazakhstan. NuDNA sequences fail to resolve relationships within this complex, yet mtDNA markers suggest the presence of three main matrilines: (1) *P. guttatus*, *P. moltschanovi*, and *P. alpheraki* from the Caspian and Aral basins and Ili Depression in eastern Kazakhstan; (2) *Phrynocephalus kuschakewitschi* Bedriaga, 1905 and *P. incertus* Bedriaga, 1905 from the Balkhash Lake Basin in eastern Kazakhstan; and (3) *Phrynocephalus melanurus* from the Zaysan Depression in northeastern Kazakhstan and Junggar Depression of northwestern China. Significant differentiation in mtDNA sequences (p=4.0–7.9% for *COI*), morphology and distribution argue for recognizing these forms of *P. guttatus* as full species. However, further research including more variable nuclear DNA-markers is necessary before doing so, especially in the Balkash Lake Basin in Eastern Kazakhstan, which cradles the highest species diversity of this group and where gene flow between species might take place (E. Solovyeva et al., 2018, Unpublished data).

Lineage I comprises the species of *P. versicolor*-group that inhabit lowland deserts of northern Central Asia. Whereas the nuDNA analyses do not resolve relationships within this group, mtDNA results suggest the presence of two matrilines, one containing populations from the Mongolian part of the Junggar Depression (Mongolian Jungaria), previously assigned to *P. versicolor hispida* (*Orlova et al., 2014*). Concatenated analysis of nuDNA loci suggest its recognition as the full species *P. hispidus* Bedriaga, 1909 **comb. et stat. nov.** The mtDNA divergence of this lineage from other members of *P. versicolor* group is substantial (p = 6.7–7.3%). Our analyses are in concordance the

previous results by *Gozdzik & Fu (2009)* and *Urquhart, Wang & Fu (2009)* on genetic uniformity of *P. przewalskii* and *P. frontalis*. Despite the presence of two matrilines, the nuDNA markers do not differ between the two and *P. przewalskii* Strauch, 1876 appears to be the senior synonym for this taxon.

Phrynocephalus versicolor is a wide-ranging species that inhabits the Mongolian and Chinese Gobi Desert as far northwards as the Tuva Republic in southern Siberia (Russia). Traditionally, two subspecies were recognized: *P. v. kulagini* from Tuva and northern Mongolia and *P. v. versicolor* from the rest of species' range. Previous studies (*Wang & Fu, 2004*) did not include samples of *P. v. kulagini*; our analyses strongly indicate paraphyly of *P. versicolor* s.l. with specimens from Tuva being significantly differentiated both in mtDNA ($p = 5.18$–5.37% for *COI*), nuDNA genes, and morphology. These results are supported by morphological differentiation (*Dunayev, 2009*), and this requires recognition of the full species *P. kulagini* Bedriaga, 1909 **comb. et. stat. nov.**

Implications for morphological and ecological evolution

Ancestral structural substrate niche. A debate exists on the ancestral habitat niche of *Phrynocephalus*. Several authors suggested that the common ancestor *Phrynocephalus* was likely adapted to soft, wind-blown sand dunes (*Chernov, 1948*; *Whiteman, 1978*; *Arnold, 1999*), whereas others argued that the group arose in stony or clay deserts with solid ground (*Ananjeva & Tuniev, 1992*; *Golubev, 1989*). *Arnold (1999)* provided a morphology-based phylogeny for *Phrynocephalus*, and with *Trapelus* and *Bufoniceps* reconstructed as its sister-taxa. He assumed that this group of genera demonstrated a gradual adaptation to soft substrates, such as loose aeolian sand-dunes.

We reconstructed the evolution of the preferred habitat types among all sampled *Phrynocephalus* and Agaminae outgroups using MP (Fig. 7; Table S6). Most Agaminae genera climb to some extent (*Arnold, 1999*) as *Agama*, *Pseudotrapelus*, and *Laudakia* s.l. exhibit. These taxa are found mostly frequently on large rocks and boulders, and this also occurs for most *Trapelus*, which inhabit sandy or gravel deserts, but eagerly climb bushes and trees. Only three genera—*Xenagama*, *Bufoniceps*, and *Phrynocephalus*—are strictly ground-dwelling, and this appears to be the derived condition. Our analysis suggests that two lineages within Agaminae independently adapted to life on soft substrates: the common ancestor of *Trapelus* and *Bufoniceps*, and the ancestor of *Phrynocephalus*.

Loose sands with non-differentiated proluvial sediments appear to be the ancestral habitat of *Phrynocephalus*. This initial adaptation could result in evolution of a set of advantageous features typical for this genus, such as (1) skin covering the tympanum, (2) lateral fringes of elongate scales on digits and eyelids, (3) countersunk jaws, (4) flattened body and tail, and (5) a characteristic burial behavior by lateral oscillations of the body (*Arnold, 1999*; *Dunayev, 1996b*). Further differentiation within *Phrynocephalus* likely led to adaptations of different lineages to contrasting habitat preferences. *Phrynocephalus* of clade I mostly specialize for life on sandy habitats such as large, wind-blown dunes (*P. mystaceus* and *P. ornatus*–*P. interscapularis* groups). Two species of clade I (*P. scutellatus* and *P. maculatus*) demark independent shifts to firmer ground (clay soils with gravel or salines). Clade II demonstrates adaptation to high elevation, stony or gravel deserts; a

reversal to sand habitats occurs for *P. forsythii*, which inhabits the sandy Taklimakan Desert at lower elevations. Clade III likely had a sand-dwelling ancestor (Fig. 7). Many species in this group live on fixed sands with patches of gravel or clay, or they can be observed on various substrates. Some species switch to wind-blown dunes (*P. axillaris, P. melanurus, P. przewalskii*) or gravel (*P. alpherakii, P. kuschakewitschi, P. melanurus, P. versicolor, P. strauchi*). All members of the *P. raddei–P. helioscopus* group are specialized to life on hard substrates (clay, gravel, salines) and show no reversal to sand habitats, with the exception of *P. helioscopus varius*, which occurs in sandy areas of pine forests in the northernmost limit of its distribution in the Altai Region of Russia (*Kotlov, 2008*).

Body size evolution. *Phrynocephalus* show significant variation in body size ranging from 35–37 mm (*P. ornatus vindumi*) to 123 mm (*P. mystaceus*) (Table S6). The weighted squared-change parsimony algorithm serves to reconstruct the evolution of maximum SVL in *Phrynocephalus* and outgroup Agaminae (Fig. 8). Accordingly, rock-dwelling or climbing forms such as *Agama, Trapelus,* and *Laudakia* s.l. have larger SVLs than strictly ground-dwelling *Bufoniceps, Xenagama,* and *Phrynocephalus.* Body size decreases early in the history of *Phrynocephalus*, suggesting that initial miniaturization of its common ancestor was advantageous in wind-blown sand habitats. Strict sand-dwellers, *Microphrynocepahlus* (*P. ornatus–P. interscapularis* group) found in the aeolian sand dunes of the Middle East and Turan are the most miniaturized group of *Phrynocephalus* (SVL_{max} 47 mm). An example of an overt reversal in body size occurs in *P. mystaceus*, which is the largest member of the genus and is also specialized to large floating sand dunes. Similar change in body size possibly took place in psammophilous *P. euptilopus*, which appears to be closely related to *P. interscapularis–P. luteoguttatus*, but is much larger (SVL_{max} 63 mm) (*Alcock & Finn, 1897; Arnold, 1999*). Some species adapted to hard substrates also show an increase in body size, such as *P. maculatus* (SVL_{max} 91 mm) and *P. putjatai* (SVL_{max} 84 mm).

Historical biogeography

Time-tree and origin of *Phrynocephalus*. Estimates of divergence and diversification times for *Phrynocephalus* vary among authors. *Macey et al. (1993)* based on allozymes assumed that *Phrynocepalus* represented an ancient radiation and diverged about 35 Ma. According to immunological data, *Ananjeva & Sokolova (1990)* estimated the divergence of *Phrynocephalus* from other Agaminae took place around 11 Ma, while their allozyme data provided an estimate of 6 Ma. Using relaxed clock dating, *Guo & Wang (2007)* suggested a mid-Miocene origin (13.87 Ma, 95% CI [8.5–20.5]). Estimates by *Melville et al. (2009)* were older and varied for mtDNA and nuDNA datasets. Their mtDNA suggested all *Phrynocephalus* including *P. interscapularis* diverged 28.9 Ma (21.1–36.2 Ma). Excluding *P. interscapularis*, the estimated origin dated to 22.4 Ma (16.5–30.6 Ma) for mtDNA, and 15.8 Ma (11.8–23.0 Ma) for nuDNA.

Our analyses based on mtDNA data suggest that the ancestor of *Phrynocephalus* diverged from other Agaminae in early Oligocene around 33.2 Ma (19.92–45.69 Ma), or based on nuDNA data in late Oligocene around 26.9 Ma (22.44–31.27 Ma). The basal differentiation within the genus took place in early Miocene (mean 19.3 Ma; 95% CI

[12.20–28.90] Ma) or mid-Miocene (mean 14.76 Ma; 95% CI [12.01–17.47] Ma) based on mtDNA and nuDNA data, respectively (Table S10). Due to absence of a reliable fossil record of *Phrynocephalus*, all of our calibration nodes correspond to relatively old splits between outgroup taxa, which can potentially result in biased date estimates (see, e.g., *Brochu, 2004*; *Hugall, Foster & Lee, 2007*).

Our estimates best fit the results of *Melville et al. (2009)*, but are slightly younger. *Melville et al. (2009)* used one biogeographic and four fossil calibrations, including the enigmatic *Bharatagama* from Early–Middle Jurassic of peninsular India, which is interpreted as a putative stem acrodont (*Evans, Prasad & Manhas, 2002*). However, the attribution of this fossil is questionable (*Townsend et al., 2011*) and our calibration scheme does not include it (Table S5).

Biogeographic history of *Phrynocephalus* and Cenozoic climate change. *Phrynocephalus* is a characteristic element of the deserts of Palearctic Asia, and there is a substantial sympatry between species and species groups (*Arnold, 1999*) (Fig. S4). Several hypotheses have been invoked to explain the current broad distribution of the genus. *Nikolsky (1916)* assumed a Central Asian or Tibetan origin based on remarkable morphological diversity of Central Asian species ("northern origin" hypothesis). *Ananjeva & Tuniev (1992)* speculated that there were two original centers for the species of *Phrynocephalus* in the former USSR: Central Asia in the north and Middle Asia in the south. However, their complex hypothesis is not based on an estimated phylogeny and it omits numerous species of *Phrynocephalus* unique to Southwest Asia and China (*Kamali & Anderson, 2015*). *Macey et al. (1993)* suggested that the origins of *Phrynocephalus* trace back to Indian collision with Eurasia 35 Ma. Later *Arnold (1999)* suggested that *Phrynocephalus* evolved in the southern margins of the present distribution, i.e., in the Arabia–NW India area rather than in Central Asia ("southern origin" hypothesis). Some researchers (*Wang & Macey, 1993*; *Zeng et al., 1997*; *Pang et al., 2003*) argued that the basal differentiation of *Phrynocephalus* and the origin of the viviparous species group resulted from vicariance associated with the uplifting of the QTP. *Guo & Wang (2007)* suggested that *Phrynocephalus* diversified in the late Miocene to Pleistocene from centers of origin in temperate deserts of Central Asia, and the Tarim and Junggar basins. Several rapid speciation events followed this in a relatively short time (northern origin hypothesis). However, despite recent progress based on molecular phylogenetics (*Pang et al., 2003*; *Melville et al., 2009*; *Guo & Wang, 2007*), our understanding of the biogeography of *Phrynocephalus*, especially of the oviparous taxa inhabiting Middle Asia and South-Western Asia, remains very poor.

Phrynocephalus belongs to the subfamily Agaminae, which is hypothesized to have originated in Afro-Arabia and colonized Eurasia during a slow closure of the Tethys following movement of Arabian plate northwards (*Macey et al., 2000*). The landbridge connecting Afro-Arabia with Eurasia (known as "*Gomphotherium*-landbridge" or GLB; Figs. 5 and 6) was formed around 18–17 Ma and it facilitated a great faunal exchange between these landmasses (*Rögl, 1998*, *1999*). After a temporary disruption, the landbridge has persisted continuously since the mid-Miocene about 15 Ma (*Harzhauser et al., 2007*; *Pook et al., 2009*; *Metallinou et al., 2012*; *Scherler et al., 2013*; *Šmíd et al., 2013*). Our

analyses strongly suggest that the ancestor of *Phrynocephalus* diverged from other agamines around 27 Ma in late Oligocene, or ca. 9–10 million years predating the first connection of Afro-Arabia with Eurasia. Because Asian agamines are not monophyletic with respect to African taxa, if *Macey et al.'s (2000, 2006)* hypothesis on an Afro-Arabian origin of the subfamily is correct, then the ancestor of *Phrynocephalus*, *Laudakia*, and *Trapelus + Bufoniceps* should have colonized Asia independently from Arabia before formation of the GLB. Because Agamidae and putative Agaminae were present in Asia starting from the late Cretaceous and early Cenozoic (*Estes, 1983*; *Borsuk-Białynicka & Moody, 1984*; *Alifanov, 1989*; *Borsuk-Białynicka, 1996*; *Prasad & Bajpai, 2008*), we cannot exclude an Asian origin of Agaminae with subsequent colonization of Africa. The oldest known fossil of *Phrynocephalus* is reported from eastern Turkey (*Zerova & Chkhikvadze, 1984*); this record is quite young quite young (ca. 5 Ma) and not reliable. The driver of the basal differentiation within Agaminae in Oligocene (ca. 29 Ma) remains an enigma, as does the distribution of the common ancestor of *Phrynocephalus* (Fig. 5).

Figure 5 shows the main events in biogeographic history of *Phrynocephalus* inferred from molecular analyses and paleorange reconstructions. The basal radiation of *Phrynocephalus* happened around 14.8 Ma and likely took place in Middle East or southern Middle Asia (Turan) (Fig. 5). This scenario cannot reject the "southern origin" hypothesis for *Phrynocephalus*, as it does for the other hypotheses.

One of the most remarkable episodes of global climate evolution during the Cenozoic is the middle Miocene climatic transition (MMCT), which occurred between 14.8 and 14.1 Ma. (*Flower & Kennett, 1994*). At that time, a major and permanent cooling trend replaced the warm and humid tropical or subtropical climate of the mid-Miocene thermal optimum (17–15 Ma; *Zachos et al., 2001*; *Böhme, 2003*). The MMCT saw an increased meridional temperature gradient that strengthened the boundaries between climatic zones and increased aridification of the mid-latitudes (*Flower & Kennett, 1994*). The MMCT was synchronous with the Paratethys salinity crisis (*Rögl, 1999*), which was a major drying of the Paratethys Sea that may have formed significant wind-blown sand and evaporitic desert areas in Middle Asia. The MMCT aridification trend facilitated the spread of drier landscapes over the Mediterranean Basin, Arabia, the Iranian Plateau, and Middle Asia and promoted dispersal of xerophilic species (*Manafzadeh, Salvo & Conti, 2014*). The basal radiation of *Phrynocephalus* into clades I–III coincides perfectly with onset of the MMCT (14.8 Ma). The increasing aridification provided a diversity of desert habitats for *Phrynocephalus* to occupy as they started to disperse out of the ancestral area in Middle East and Turan (Fig. 5). A similar pattern was recently shown for agamid fan-throated lizards (genus *Sitana* Cuvier, 1829), which diversified in response to ongoing aridification of the Indian subcontinent in the late Miocene (*Deepak & Karanth, 2018*).

The ancestors of viviparous *Oreosaura* (clade II) supposedly colonized the QTP 13.5–10.0 Ma and diversification within this clade began around 3.8 Ma ago (Figs. 5 and 6). Our estimated divergence for *Oreosaura* is older than the earlier estimate of 9.7 Ma (95% interval: 7.2–13.0 Ma) by *Jin & Brown (2013)*. Our date coincides with hypothesized major uplifting of the QTP (*Shackleton & Chang, 1988*) and, thus, is consistent with the view that viviparity evolved when this clade became restricted to

regions of high elevation. The orogenesis of Tibet is traditionally regarded as the main driving force of Asian monsoons system and subsequent cooling and progressive aridization in Central Asia (*Ramstein et al., 1997*). However, recent works raise a doubt on the Miocene uplifting of the QTP, suggesting that Tibet has been 4–5 km high since the mid-Eocene (ca. 40 Ma), while Indian and Southeast Asian summer monsoons, and Central Asian winter monsoons arose at different times and are unrelated to Tibetan orogenesis (reviewed by *Renner, 2016*). These new data necessitate significant reconsideration of QTP historical biogeography and *Phrynocephalus* may represent a promising model group for such studies.

Oviparous clades I and III remained largely within the hypothetical ancestral range of *Phrynocephalus* (Middle East and Turan) (Figs. 5 and 6). Clade I has its highest diversity in the Iranian Plateau and adjacent parts of the Middle East. The ancestor of *P. mystaceus* diverged around 11.3 Ma; this large-sized psammophilous species spread northwards to Turan, Middle Asia and the Caspian Basin where vast areas of wind-blown sand deserts were formed after gradual drying up of the Paratethys Sea. Simultaneously, an ancestor of the *P. arabicus*–*P. maculatus* group occupied deserts of the Arabian Peninsula between 10 and 5 Ma (Fig. 5). The vicariant divergence between the ancestor of *P. arabicus* + *P. longicaudatus* from the Near East and Iranian *P. maculatus* happened around 4.8 Ma. This coincides with intensive uplifting of the Zagros Mountains in western Iran around 7 to 5 Ma ago (*Mouthereau, Lacombe & Vergés, 2012*).

Oviparous clade III encompasses the highest number of species and has the largest distribution in ranging from the Middle East and Asia Minor to Turan and Middle and Central Asia. Cladogenesis started in the late Miocene (ca. 8.9–7.1 Ma) and was likely influenced by progressive aridification of central Eurasia, orogenesis and changes in level of the Paratethys Sea. The age of the Central Asian deserts is questionable. The 22 Ma estimation of the onset of aridification in northwestern China (*Xia & Hu, 1993*; *Guo et al., 2002*) corresponds with estimates for the basal radiation in Dipodidae (*Shenbrot et al., 2017*), which is the major autochthonous component of Central Asian desert mammal community. The primary center of radiation for *Phrynocephalus* in Southwest Asia best explains their apparent lag in radiation.

The *P. raddei*–*P. helioscopus* group adapted to life on gravel or clay deserts. The highest diversity within this group occurs on alluvial plains of Middle Asia and Turan. The *P. helioscopus*–*P. persicus* species complex has largest distribution penetrating westwards to Transcaucasia and eastern Asia Minor, and northwards to the Caspian Basin, lowland deserts of Middle and Central Asia as far as western Mongolia (Fig. 5). Orogenetic processes in the Iranian Plateau and Kopet Dagh Mountains (*Smit et al., 2013*) possibly shaped the initial splits (6.2–3.4 Ma). The common ancestor of the *P. axillaris* and *P. guttatus*–*P. versicolor* group likely dispersed to Central Asia around 8.5 to 7 Ma, where it diversified. Accordingly, *P. axillaris* appears to have remained in the Taklimakan Basin and adjacent parts of Tibet, where desertification started from at least 22.6 Ma ago (*Zheng et al., 2015*). The ancestors of the *P. guttatus*–*P. versicolor* group penetrated to Middle Asia (*Dunayev, 2009*). Divergence between *P. guttatus* and *P. versicolor* species complexes occurred around 3.8 Ma, and this may coincide with accelerated uplifting of the Altai and

Tianshan mountains around 5.0 to 3.1 Ma (*Avouac et al., 1993*; *Abdrakhmatov et al., 1996*; *Charreau et al., 2005*; *Yuan et al., 2006*). The ancestors of *P. guttatus* and *P. moltschanovi* further spread westwards, occupying the Caspian Basin and north-western Turan (Fig. 5).

Plio–Pleistocene glacial cycling likely profoundly affected subsequent radiations and range expansions within species complexes occupying northern parts of Middle and Central Asia (*Aubekerov & Gorbunov, 1999*). Formation of local montane glaciers or permafrost areas during glacial maximums could have led to the retreat of *Phrynocephalus* to warmer refugia followed by subsequent dispersals in warmer periods (*Melville et al., 2009*). Apparently, the QTP, now home to an impressive radiation of viviparous *Oreosaura*, was covered by a thick ice sheet in the Pleistocene (*Kuhle, 1998*). Hence, their distributions and the role they played in shaping the Central Asian biota remains insufficiently understood and requires further studies.

CONCLUSIONS

Exhaustive taxonomic sampling of *Phrynocephalus* is challenging. Some species of *Phrynocephalus* are only known from the type specimens and old collections (e.g., *P. euptilopus* and *P. nasatus*) (*Barabanov & Ananjeva, 2007*), while others occur in politically unstable zones (e.g., deserts of Pakistan, Afghanistan, and Taklamakan). Our analyses provide the most comprehensive taxonomic and gene sampling for *Phrynocephalus* to date. We evaluate 32 nominal taxa using four mtDNA and four nuDNA protein-coding genes. The sampling comprises over four-fifths of the species and covers the distribution of the genus. The mtDNA and nuDNA trees clarify the initial cladogenesis of these lizards. Statistically significant mito-nuclear discordance occurs likely due to hybridization and the introgression of mitogenomes. Analyses shed light on a number of taxonomic issues. Our results contribute to the interpretation of diversification patterns of Central Asian arid zone lizards and provides insights into the historical biogeography of this region.

Analyses confirm the monophyly of *Phrynocephalus* and infer its biogeographic history. The ancestral area of the Agaminae and factors that influenced its diversification remains uncertain. The origin of *Phrynocephalus* dates to the late Oligocene (26.9 Ma) and this precedes the formation of the mid-Miocene landbridge that connected Africa and Asia. The common ancestor of *Phrynocephalus* appears to have been a ground-dwelling, miniaturized agamine adapted to sand habitats. The basal divergence of *Phrynocephalus* into three major clades appears to have occurred in the Middle East or southern Middle Asia (Turan) around 14.8 Ma. This corresponds well with the mid-Miocene climatic transition—climate cooling that coincided with aridification and spreading of xerophytic plants across Mediterranean and Paratethys Basins. Subsequent drying up of the Paratethys Sea formed vast desert habitats that *Phrynocephalus* appears to have occupied. Two oviparous clades dispersed independently to lowland deserts of the Arabian Peninsula, Middle and Central Asia. Orogenetic processes and Paratethys Basin dynamics appear to have driven further cladogenesis, which Pliocene–Pleistocene climate oscillations built upon. Substantial variation in body size and morphology occurs in the oviparous lizards. Viviparous *Oreosaura* occupied the QTP around 13.5–10 Ma.

Cladogenesis in this group dates between the late Oligocene and mid-Pliocene depending on the dataset (3.8 Ma from nuDNA, 6.4 Ma from mtDNA). This estimate coincides well with the divergence time of another viviparous group of lizards inhabiting Central Asia—the racerunner subgenus *Pareremias* (Lacertidae) (*Orlova et al., 2017*), which was dated to about 6.3 Ma from mtDNA data (*Guo et al., 2011*).

Climatic changes during the Cenozoic, including the ongoing aridification of central Eurasia, shaped the biodiversity of the region (*Peng et al., 2006*; *Yang et al., 2006*; *Jin, Brown & Liu, 2008*; *Melville et al., 2009*; *Guo et al., 2011*; *Jin & Brown, 2013*; *Pisano et al., 2015*). Most recent biogeographic studies assume the hypothesis that speciation in Central Asia correlated with the evolution of an East Asian monsoon climate triggered by the rapid uplifting of the QTP (*Harrison et al., 1992*, *1995*; *Zhisheng et al., 2001*; *Molnar, 2005*). However, biogeographic histories of many taxa, including those inhabiting Central Asia and the QTP, might require reconsideration due to conflicting hypotheses on geological and climatic history of the region (*Renner, 2016*). Accordingly, our study highlights the importance of Cenozoic paleogeographic and paleoclimatic events in the diversification of Palaearctic lizards.

ACKNOWLEDGEMENTS

ADDITIONAL INFORMATION AND DECLARATIONS

Funding

Grant Disclosures

Competing Interests

The authors declare that they have no competing interests.

Author Contributions

- Evgeniya N. Solovyeva conceived and designed the experiments, performed the experiments, analyzed the data, contributed reagents/materials/analysis tools, prepared figures and/or tables, authored or reviewed drafts of the paper, approved the final draft, discussion of the results.
- Vladimir S. Lebedev conceived and designed the experiments, performed the experiments, analyzed the data, authored or reviewed drafts of the paper, approved the final draft, discussion of the results.
- Evgeniy A. Dunayev conceived and designed the experiments, contributed reagents/ materials/analysis tools, authored or reviewed drafts of the paper, approved the final draft, discussion of the results.
- Roman A. Nazarov conceived and designed the experiments, contributed reagents/ materials/analysis tools, prepared figures and/or tables, authored or reviewed drafts of the paper, approved the final draft, discussion of the results.
- Anna A. Bannikova conceived and designed the experiments, authored or reviewed drafts of the paper, approved the final draft, discussion of the results.
- Jing Che conceived and designed the experiments, contributed reagents/materials/ analysis tools, authored or reviewed drafts of the paper, approved the final draft, discussion of the results.
- Robert W. Murphy conceived and designed the experiments, authored or reviewed drafts of the paper, approved the final draft, discussion of the results.
- Nikolay A. Poyarkov conceived and designed the experiments, analyzed the data, contributed reagents/materials/analysis tools, prepared figures and/or tables, authored or reviewed drafts of the paper, approved the final draft, discussion of the results.

Animal Ethics

The following information was supplied relating to ethical approvals (i.e., approving body and any reference numbers):

No experiments were conducted on living animals; only museum collections were used for this work.

DNA Deposition

The following information was supplied regarding the deposition of DNA sequences:

Sequences of AKAP9, BDNF, NKTR, and RAG-1 genes presented here are accessible via GenBank accession numbers KJ363400–KJ363439, KJ363514–KJ363551.

Data Availability

The following information was supplied regarding data availability:

Specimens examined in this study are deposited in herpetological collections of the following museums:

1. Zoological Museum of Moscow University (ZMMU, Moscow, Russia);
2. Institute of Zoology and Parasitology, Uzbek Academy of Sciences (IZIP, Tashkent, Uzbekistan);
3. Kunming Institute of Zoology, Chinese Academy of Sciences (KIZ, Kunming, Yunnan, Peoples' Republic of China).

Supplemental Information

Supplemental information for this article can be found online at http://dx.doi.org/10.7717/peerj.4543#supplemental-information.

REFERENCES

Abdrakhmatov KY, Aldazhanov SA, Hager BH, Hamburger MW, Herring TA, Kalabaev KB, Makarov VI, Molnar P, Panasyuk SV, Prilepin MT, Reilinger RE, Sadybakasov IS, Souter BJ, Trapeznikov YA, Tsurkov VY, Zubovich AV. 1996. Relatively recent construction of the Tien Shan inferred from GPS measurements of present-day crustal deformation rates. *Nature* **384(6608)**:450–453 DOI 10.1038/384450a0.

Alcock AW, Finn F. 1897. An account of the Reptilia collected by Dr. F.P. Maynard, Captain A.H. McMahon, C.I.E., and the members of the Afghan–Baluch Boundary Commission of 1896. *Journal of the Asiatic Society of Bengal* **65**:550–566.

Alifanov VR. 1989. New Priscagamida [sic] (Lacertilia) from the Upper Cretaceous of Mongolia and their systematic position among Iguania. *Paleontological Journal* **1989**:68–80.

Ananjeva NB. 1987. On the validity of *Megalochilus mystaceus* (Pallas, 1776). In: Ananjeva NB, Borkin LJ, eds. *Systematics and Ecology of Amphibians and Reptiles. Proceedings of the Zoological Institute, USSR Academy of Sciences, Leningrad.* Vol. 157, 4–13 [in Russian].

Ananjeva NB, Orlov NL, Khalikov RG, Darevsky IS, Ryabov SA, Barabanov AV. 2006. *The Reptiles of Northern Eurasia.* Sofia: Pensoft Publishers, 245.

Ananjeva NB, Sokolova TM. 1990. The position of the genus *Phrynocephalus* Kaup 1825 in agamids system. *Trudy Zoologicheskogo Instituta Akademii Nauk SSSR* **207**:12–21.

Ananjeva NB, Tuniev BS. 1992. Historical biogeography of the *Phrynocephalus* species of the USSR. *Asiatic Herpetological Research* **4**:76–98.

Arévalo E, Davis SK, Sites JW Jr. 1994. Mitochondrial DNA sequence divergence and phylogenetic relationships among eight chromosome races of the *Sceloporus grammicus* complex (Phrynosomatidae) in central Mexico. *Systematic Biology* **43(3)**:387–418 DOI 10.1093/sysbio/43.3.387.

Arnold EN. 1992. The Radjasthan toad-headed lizard, *Phrynocephalus longwalensis* (Reptilia: Agamidae) represents a new genus. *Journal of Herpetology* **26(4)**:467–472 DOI 10.2307/1565125.

Arnold EN. 1999. Phylogenetic relationships of toad-headed lizards (*Phrynocephalus*, Agamidae) based on morphology. *Bulletin of the British Museum (Natural History)* **65(1,3)**:1–13.

Aubekerov B, Gorbunov A. 1999. Quaternary permafrost and mountain glaciation in Kazakhstan. *Permafrost and Periglacial Processes* **10(1)**:65–80 DOI 10.1002/(sici)1099-1530(199901/03)10:13.0.co;2-x.

Avouac J-P, Tapponnier P, Bai M, You H, Wang G. 1993. Active thrusting and folding along the northern Tien Shan and late Cenozoic rotation of the Tarim relative to Dzungaria and Kazakhstan. *Journal of Geophysical Research* **98(B4)**:6755–6804 DOI 10.1029/92jb01963.

Bannikov AG, Darevsky IS, Ischchenko VG, Rustamov AK, Szczerbak NN. 1977. *Opredelitel Zemnovodnikh i Presmikayushchikhsya Fauni SSSR [Guide to the Reptile and Amphibian Fauna of the USSR]*. Moscow: Enlightenment Publ., 414 [in Russian].

Barabanov AV, Ananjeva NB. 2007. Catalogue of the available scientific species-group names for lizards of the genus *Phrynocephalus* Kaup, 1825 (Reptilia, Sauria, Agamidae). *Zootaxa* **1399(1)**:1–56 DOI 10.11646/zootaxa.1399.1.1.

Boettger O. 1888. Über die Reptilien und Batrachier Transcaspiens. In: Zoologischer A, ed. Vol. 11. Jena: VEB Gustav Fischer Verlag, 259–263.

Böhme M. 2003. The Miocene climatic optimum: evidence from ectothermic vertebrates of Central Europe. *Palaeogeography, Palaeoclimatology, Palaeoecology* **195(3–4)**:389–401 DOI 10.1016/S0031-0182(03)00367-5.

Borsuk-Białynicka M. 1996. The Late Cretaceous lizard *Pleurodontagama* and the origin of tooth permanency in Lepidosauria. *Acta Palaeontologica Polonica* **41(3)**:231–252.

Borsuk-Białynicka M, Moody SM. 1984. Priscagaminae, a new subfamily of the Agamidae (Sauria) from the Late Cretaceous of the Gobi Desert. *Acta Palaeontica Polonica* **29**:51–81.

Brochu CA. 2004. Calibration age and quartet divergence date estimation. *Evolution* **58(6)**:1375–1382 DOI 10.1554/03-509.

Burland TG. 1999. DNASTAR's lasergene sequence analysis software. *Methods in Molecular Biology* **132**:71–91 DOI 10.1385/1-59259-192-2:71.

Cerling TE, Harris JM, MacFadden BJ, Leakey MG, Quade J, Eisenmann V, Ehleringer JR. 1997. Global vegetation change through the Miocene/Pliocene boundary. *Nature* **389(6647)**:153–158 DOI 10.1038/38229.

Charreau J, Chen Y, Gilder S, Dominguez S, Avouac J-P, Sen S, Sun D, Li Y, Wang W-M. 2005. Magnetostratigraphy and rock magnetism of the Neogene Kuitun He section (northwest China): implications for Late Cenozoic uplift of the Tianshan Mountains. *Earth and Planetary Science Letters* **230(1–2)**:177–192 DOI 10.1016/j.epsl.2004.11.002.

Chernov SA. 1948. Reptiles—Reptilia. In: Pavlovsky EN, Vinogradova BS, eds. *The Animals of the USSR. Vol. 2. The Desert Zone*. Moscow: Published by USSR Academy of Sciences, 127–161 [in Russian].

Chernov SA. 1959. Reptilia. Fauna of Tajik USSR. *Dushanbe* **48**:203.

Clemann N, Melville J, Ananjeva NB, Scroggie MP, Milto K, Kreuzberg E. 2008. Microhabitat occupation and functional morphology of four species of sympatric agamid lizards in the Kyzylkum Desert, central Uzbekistan. *Animal Biodiversity and Conservation* **31(2)**:1–1.

Deepak V, Karanth P. 2018. Aridification driven diversification of fan-throated lizards from the Indian subcontinent. *Molecular Phylogenetics and Evolution* **120(2018)**:53–62 DOI 10.1016/j.ympev.2017.11.016.

Drummond AJ, Suchard MA, Xie D, Rambaut A. 2012. Bayesian phylogenetics with BEAUti and the BEAST 1.7. *Molecular Biology and Evolution* **29(8)**:1969–1973 DOI 10.1093/molbev/mss075.

Dunayev EA. 1995. Reviewed description of the types of *Phrynocephalus strauchi* Nikolsky, 1899 (Squamata, Agamidae) and materials on the history of its study, distribution, and variability. *Russian Journal of Herpetology* **2(2)**:87–94.

Dunayev EA. 1996a. Nomenclature and distribution of toad-agamas, *Phrynocephalus* (Reptilia, Agamidae) in Iliyskaya Hollow. *Bulletin of the Moscow Society of Naturalists, Biology Series, Moscow* **101(3)**:36–41.

Dunayev EA. 1996b. On the possible use of the ethological features in the taxonomy and phylogeny of toad agamas. *Russian Journal of Herpetology* **3(1)**:32–38.

Dunayev EA. 2008. Phylogeny of lizards of Phrynocephalus genus (Reptilia: Agamidae): history of study and methodic approaches. In: *Voprosy Gerpetologii*. Moscow: Zoological Museum, Moscow State University, 105–114.

Dunayev EA. 2009. Systematics and paleogeography: conceptual synthesis by the example of *Phrynocephalus* (superspecies *guttatus*) (Reptilia: Agamidae). In: Sviridov AV, Shatalkin AI, eds. *Evolution and Systematics: Lamarck and Darwin in Modern Studies. Archiver of the Zoological Museum of Moscow State University.* Vol. L. Moscow: KMK Scientific Press, 274–298 [in Russian].

Eichwald DE. 1831. Zoologia specialis quam expozitis animalibus tum vivis, tum fossilibus potissimus rossiae in universum, et poloniae in species. In: *Posterior, Specialem Expositionem Spondylozoorum Continens.* Vilnae: J. Zawadzki, 404.

Eremchenko V, Panfilov A. 1999. Some question of methodology of taxonomy and phylogeny of toad agamas on the example of *Phrynocephalus helioscopus* (Pallas, 1771) (Sauria: Agamidae). *Nauka i Noviye Tekhnologii, Bishkek* **3**:116–122.

Estes R. 1983. *Sauria Terrestria, Amphisbaenia (Handbuch der Paläoherpetologie, v. 10A).* Stuttgart: Gustav Fischer Verlag, 249.

Evans SE, Prasad GVR, Manhas BK. 2002. Fossil lizards from the Jurassic Kota formation of India. *Journal of Vertebrate Paleontology* **22(2)**:299–312 DOI 10.1671/0272-4634(2002)022[0299:FLFTJK]2.0.CO;2.

Farris JS, Kallersjo M, Kluge AG, Bult C. 1994. Testing significance of incongruence. *Cladistics* **10(3)**:315–319 DOI 10.1111/j.1096-0031.1994.tb00181.x.

Farris JS, Kallersjo M, Kluge AG, Bult C. 1995. Constructing a significance test for incongruence. *Systematic Biology* **44(4)**:570–572 DOI 10.1093/sysbio/44.4.570.

Felsenstein J. 2004. *Inferring Phylogenies.* Vol. 2. Sunderland: Sinauer Associates, Inc., 465.

Fisher-Reid MC, Wiens JJ. 2011. What are the consequences of combining nuclear and mitochondrial data for phylogenetic analysis? Lessons from *Plethodon* salamanders and 13 other vertebrate clades. *BMC Evolutionary Biology* **11(1)**:300 DOI 10.1186/1471-2148-11-300.

Flower BP, Kennett JP. 1994. The middle Miocene climatic transition: East Antarctic ice sheet development, deep ocean circulation and global carbon cycling. *Palaeogeography, Palaeoclimatology, Palaeoecology* **108(3–4)**:537–555 DOI 10.1016/0031-0182(94)90251-8.

Golonka J. 2004. Plate tectonic evolution of the southern margin of Eurasia in the Mesozoic and Cenozoic. *Tectonophysics* **381(1–4)**:235–273 DOI 10.1016/j.tecto.2002.06.004.

Golubev ML. 1989. Three controversial questions of systematics and nomenclature in Phrynocehpahlus of USSR fauna (Phrynocephalus, Agamidae). *Questions of Herpetology: Abstracts of the 7th Conference, Kiev,* 44–45. [in Russian].

Golubev ML. 1991. About the name *Agama* ocellata Lichtenstein in Eversmann, 1823 (Reptilia, Agamidae) with redescription of the types. *Herpetological Researches* **1**:12–17.

Golubev ML. 1993. The variegated toad agama in Djungar Gate (Eastern Kazakstan) with notes on certain systematic problems of *Phrynocephalus versicolor* str. (Reptilia: Agamidae). *Asiatic Herpetological Research* **5**:51–58.

Golubev ML, Gorelov YK, Dunayev EA, Kotenko TI. 1995. On the finding of *Phrynocephalus guttatus* (Gmel.) (Sauria, Agamidae) in Turkmeniya and its taxonomic status. *Bulletin of the Moscow Society of Naturalists [Bulleten Moskovskogo Obschestva Ispytateley Prirody], Otdel Biologicheskiy* **100(3)**:31–39.

Gozdzik A, Fu J. 2009. Are toad-headed lizards *Phrynocephalus przewalskii* and *P. frontalis* (family Agamidae) the same species? Defining species boundaries with morphological and molecular data. *Russian Journal of Herpetology* **16(2)**:107–118.

Guo X, Dai X, Chen D, Papenfuss T, Ananjeva NB, Melnikov DA, Wang Y. 2011. Phylogeny and divergence times of some racerunner lizards (Lacertidae: Eremias) inferred from mitochondrial 16S rRNA gene segments. *Molecular Phylogenetics and Evolution* **61(2)**:400–412 DOI 10.1016/j.ympev.2011.06.022.

Guo ZT, Ruddiman WF, Hao QZ, Wu HB, Qiao YS, Zhu RX, Peng SZ, Wei JJ, Yuan BY, Liu TS. 2002. Onset of Asian desertification by 22 Myr ago inferred from loess deposits in China. *Nature* **416(6877)**:159–163 DOI 10.1038/416159a.

Guo X, Wang Y. 2007. Partitioned Bayesian analyses, dispersal-vicariance analysis, and the biogeography of Chinese toad-headed lizards (Agamidae: Phrynocephalus): a re-evaluation. *Molecular Phylogenetics and Evolution* **45(2)**:643–662 DOI 10.1016/j.ympev.2007.06.013.

Haas G. 1957. Some amphibians and reptiles from Arabia. *Proceedings of the California Academy of Sciences* **29(3)**:47–86.

Hall TA. 1999. BioEdit: a user-friendly biological sequence alignment editor and analysis program for Windows 95/98/NT. *Nucleotide* **41**:95–98.

Harrison TM, Copeland P, Kidd WSF, Lovera OM. 1995. Activation of the Nyainqentanghla shear zone: implications for uplift of the southern Tibetan Plateau. *Tectonics* **14(3)**:658–676 DOI 10.1029/95TC00608.

Harrison TM, Copeland P, Kidd WSF, Yin A. 1992. Raising Tibet. *Science* **255(5052)**:1663–1670 DOI 10.1126/science.255.5052.1663.

Harzhauser M, Kroh A, Mandic O, Piller WE, Göhlich U, Reuter M, Berning B. 2007. Biogeographic responses to geodynamics: a key study all around the Oligo-Miocene Tethyan Seaway. *Zoologischer Anzeiger* **246(4)**:241–256 DOI 10.1016/j.jcz.2007.05.001.

Heled J, Drummond AJ. 2010. Bayesian inference of species trees from multilocus data. *Molecular Biology and Evolution* **27(3)**:570–580 DOI 10.1093/molbev/msp274.

Huelsenbeck JP, Hillis DM. 1993. Success of phylogenetic methods in the four-taxon case. *Systematic Biology* **42(3)**:247–264 DOI 10.1093/sysbio/42.3.247.

Huelsenbeck JP, Ronquist F. 2001. MrBayes: Bayesian inference of phylogenetic trees. *Bioinformatics* **17**:754–755.

Hugall AF, Foster R, Lee MSY. 2007. Calibration choice, rate smoothing, and the pattern of tetrapod diversification according to the long nuclear gene RAG-1. *Systematic Biology* **56(4)**:543–563 DOI 10.1080/10635150701477825.

International Code of Zoological Nomenclature (ICZN). 1999. *International Code of Zoological Nomenclature.* Fourth Edition. London: The International Trust for Zoological Nomenclature.

Ivanova NV, DeWaard JR, Hebert PDN. 2006. An inexpensive, automation friendly protocol for recovering high quality DNA. *Molecular Ecology Notes* **6(4)**:998–1002 DOI 10.1111/j.1471-8286.2006.01428.x.

Jin Y-T, Brown RP. 2013. Species history and divergence times of viviparous and oviparous Chinese toad-headed sand lizards *(Phrynocephalus)* on the Qinghai-Tibetan Plateau. *Molecular Phylogenetics and Evolution* **68(2)**:259–268 DOI 10.1016/j.ympev.2013.03.022.

Jin Y-T, Brown RP, Liu N-F. 2008. Cladogenesis and phylogeography of the lizard *Phrynocephalus vlangalii* (Agamidae) on the Tibetan Plateau. *Molecular Ecology* **17(8)**:1971–1982 DOI 10.1111/j.1365-294X.2008.03721.x.

Jin Y-T, Liu N-F. 2010. Phylogeography of *Phrynocephalus erythrurus* from the Qiangtang Plateau of the Tibetan Plateau. *Molecular Phylogenetics and Evolution* **54(3)**:933–940 DOI 10.1016/j.ympev.2009.11.003.

Jin Y, Liu N, Brown RP. 2017. The geography and timing of genetic divergence in the lizard Phrynocephalus theobaldi on the Qinghai-Tibetan Plateau. *Scientific Reports* **7(1)**:2281 DOI 10.1038/s41598-017-02674-4.

Jobb G. 2011. TREEFINDER: March 2011. *Available at* www.treefinder.de.

Kamali K, Anderson SC. 2015. A new Iranian *Phrynocephalus* (Reptilia: Squamata: Agamidae) from the hottest place on earth and a key to the genus *Phrynocephalus* in southwestern Asia and Arabia. *Zootaxa* **3904(2)**:249–260 DOI 10.11646/zootaxa.3904.2.4.

Kotlov AA. 2008. Species composition and distribution of amphibians and reptiles of south-western Kulunda. *Altaiskiy Zoologicheskiy Zhurnal* **2**:131–133.

Kuhle M. 1998. Reconstruction of the 2.4 million km^2 late Pleistocene ice sheet on the Tibetan Plateau and its impact on the global climate. *Quaternary International* **45**:71–108 DOI 10.1016/s1040-6182(97)00008-6.

Lanfear R, Calcott B, Ho SYW, Guindon S. 2012. PartitionFinder: combined selection of partitioning schemes and substitution models for phylogenetic analyses. *Molecular Biology and Evolution* **29(6)**:1695–1701 DOI 10.1093/molbev/mss020.

Leache AD, Cole CJ. 2007. Hybridization between multiple fence lizard lineages in an ecotone: locally discordant variation in mitochondrial DNA, chromosomes, and morphology. *Molecular Ecology* **16(5)**:1035–1054 DOI 10.1111/j.1365-294X.2006.03194.x.

Likhnova O. 1992. Biochemical systematics of toad agamas *Phrynocephalus* (Agamidae, Reptilia). In: *Asian Herpetological Meeting*, Huangshan, 46–47.

Lomolino MV, Sax DF, Riddle BR, Brown JH. 2006. The island rule and a research agenda for studying ecogeographical patterns. *Journal of Biogeography* **33(9)**:1503–1510 DOI 10.1111/j.1365-2699.2006.01593.x.

Ma C, Arias EF, Eubanks TM, Fey AL, Gontier A-M, Jacobs CS, Sovers OJ, Archinal BA, Charlot P. 1998. The international celestial reference frame as realized by very long baseline interferometry. *Astronomical Journal* **116(1)**:5–6 DOI 10.1086/300408.

Macey JR, Ananjeva NB, Zhao EM, Wang YZ, Papenfuss TJ. 1993. An allozyme-based phylogenetic hypothesis for *Phrynocephalus* (Agamidae) and its implications for the historical biogeography of arid Asia. In: *Proceedings of the First Asian Herpetological Meeting*, Beijing: China Forestry Press, 349.

Macey JR, Schulte JA II, Fong JJ, Das I, Papenfuss TJ. 2006. The complete mitochondrial genome of an agamid lizard from the Afro-Asian subfamily Agaminae and the phylogenetic position of *Bufoniceps* and *Xenagama*. *Molecular Phylogenetics and Evolution* **39(3)**:291–297 DOI 10.1016/j.ympev.2005.08.020.

Macey JR, Schulte JA II, Larson A, Ananjeva NB, Wang Y, Rastegar-Pouyani N, Pethiyagoda R, Papenfuss TJ. 2000. Evaluating Trans-Tethys migration: an example using acrodont lizard phylogenetics. *Systematic Biology* **49(2)**:233–256 DOI 10.1093/sysbio/49.2.233.

Maddison WP. 1991. Squared-change parsimony reconstructions of ancestral states for continuous-valued characters on a phylogenetic tree. *Systematic Zoology* **40(3)**:304–314 DOI 10.2307/2992324.

Maddison WP, Maddison DR. 2017. Mesquite: a modular system for evolutionary analysis. Version 3.31. *Available at* http://mesquiteproject.org.

Manafzadeh S, Salvo G, Conti E. 2014. A tale of migrations from east to west: the Irano-Turanian floristic region as a source of Mediterranean xerophytes. *Journal of Biogeography* **41(2)**:366–379 DOI 10.1111/jbi.12185.

Manilo VV. 2000. Description of karyotypes of some species and subspecies of the genus *Phrynocephalus* (Sauria, Agamidae) from Central Asia. *Vestnik Zoologii* **34(6)**:113–118.

Manilo VV. 2001. Cytogenetic review and evolution of karyotypes in the species of the genus *Phrynocephalus* Kaup, 1825 (Sauria, Agamidae) from the Eastern Palaearctic. *Hamadryad* **26(2)**:227–234.

Manilo VV, Golubev ML. 1993. Karyotype information on some toad agamas of the *Phrynocephalus* species group (Sauria, Agamidae) of the former USSR. *Asiatic Herpetological Research* **5**:105–108.

McGuire JA, Linkem CW, Koo MS, Hutchison DW, Lappin AK, Orange DI, Lemos-Espinal J, Riddle BR, Jaeger JR. 2007. Mitochondrial introgression and incomplete lineage sorting through space and time: phylogenetics of crotaphytid lizards. *Evolution* **61(12)**:2879–2897 DOI 10.1111/j.1558-5646.2007.00239.x.

Melnikov DA, Melnikova E, Nazarov R, Rajabizadeh M, Al-Johany A, Amr ZS, Ananjeva NB. 2014. Taxonomic revision of *Phrynocephalus arabicus* Anderson, 1984 [sic] complex with description of a new species from Ahvaz, southwestern Iran. *Russian Journal of Herpetology* **21(2)**:149–159.

Melville J, Hale J, Mantziou G, Ananjeva NB, Milto K, Clemann N. 2009. Historical biogeography, phylogenetic relationships and intraspecific diversity of agamid lizards in the Central Asian deserts of Kazakhstan and Uzbekistan. *Molecular Phylogenetics and Evolution* **53(1)**:99–112 DOI 10.1016/j.ympev.2009.05.011.

Metallinou M, Arnold EN, Crochet PA, Geniez P, Brito JC, Lymberakis P, Baha El Din S, Sindaco R, Robinson M, Carranza S. 2012. Conquering the Sahara and Arabian deserts: systematics and biogeography of *Stenodactylus* geckos (Reptilia: Gekkonidae). *BMC Evolutionary Biology* **12(1)**:258 DOI 10.1186/1471-2148-12-258.

Molnar P. 2005. Mio-Pliocene growth of the Tibetan Plateau and evolution of East Asian climate. *Palaeontologia Electronica* **8(1)**:1–23.

Moody SM. 1980. Phylogenetic and historical biogeographical relationships of the genera in the family Agamidae (Reptilia: Lacertilia). PhD thesis, Ann Arbor, Univ Michigan, 373.

Mouthereau F, Lacombe O, Vergés J. 2012. Building the Zagros collisional orogen: timing, strain distribution and the dynamics of Arabia/Eurasia Plate convergence. *Tectonophysics* **532–535**:27–60 DOI 10.1016/j.tecto.2012.01.022.

Ng J, Glor RE. 2011. Genetic differentiation among populations of a Hispaniolan trunk anole that exhibit geographical variation in dewlap colour. *Molecular Ecology* **20(20)**:4302–4317 DOI 10.1111/j.1365-294X.2011.05267.x.

Nguyen SN, Zhou W-W, Le T-NT, Tran A-DT, Jin J-Q, Vo BD, Nguyen LT, Nguyen TT, Nguyen TQ, Hoang DD, Orlov NL, Che J, Murphy RW, Zhang Y-P. 2017. Cytonuclear discordance, cryptic diversity, complex histories, and conservation needs in Vietnamese bent-toed geckos of the *Cyrtodactylus irregularis* species complex. *Russian Journal of Herpetology* **24(2)**:133–154.

Nikolsky AM. 1916. *Reptilia. Vol. II. Ophidia. The fauna of Russia and Adjacent Countries.* Petrograd: Imperial Academy of Science Press [in Russian].

Noble DWA, Qi Y, Fu J. 2010. Species delineation using Bayesian model-based assignment tests: a case study using Chinese toad-headed agamas (genus *Phrynocephalus*). *BMC Evolutionary Biology* **10(1)**:197 DOI 10.1186/1471-2148-10-197.

Orlova VF, Dunayev EA, Nazarov RA, Terbish KH, Erdentushig P. 2014. Materials on the south-western Mongolia herpetofauna. *Sovremennaya Herpetologiya* **14(1/2)**:32–43.

Orlova VF, Poyarkov NA, Chirikova MA, Nazarov RA, Munkhbayar M, Munkhbayar KH, Terbish KH. 2017. MtDNA differentiation and taxonomy of Central Asian racerunners of Eremias multiocellata-E. przewalskii species complex (Squamata, Lacertidae). *Zootaxa* **4282(1)**:1–42 DOI 10.11646/zootaxa.4282.1.1.

Pallas PS. 1776. Reise durch verschiedene Provinzen des Russischen Reichs. St. Petersburg: Kaiserlischen Akademie der Wissenschaften.

Pang J, Wang Y, Zhong Y, Hoelzele AR, Papenfuss TJ, Zeng X, Ananjeva NB, Zhang YP. 2003. A phylogeny of Chinese species in the genus *Phrynocephalus* (Agamidae) inferred from mitochondrial DNA sequences. *Molecular Phylogenetics and Evolution* **27(3)**:398–409 DOI 10.1016/s1055-7903(03)00019-8.

Pedall I, Fritz U, Stuckas H, Valdeon A, Wink M. 2010. Gene flow across secondary contact zones of the Emys orbicularis complex in the western Mediterranean and evidence for extinction and re-introduction of pond turtles on Corsica and Sardinia (Testudines: Emydidae). *Journal of Zoological Systematics and Evolutionary Research* **49(1)**:44–57 DOI 10.1111/j.1439-0469.2010.00572.x.

Peng Z, Ho SYW, Zhang Y, He S. 2006. Uplift of the Tibetan plateau: evidence from divergence times of glyptosternoid catfishes. *Molecular Phylogenetics and Evolution* **39(2)**:568–572 DOI 10.1016/j.ympev.2005.10.016.

Pisano J, Condamine FL, Lebedev V, Bannikova A, Quéré JP, Shenbrot GI, Pages M, Michaux JR. 2015. Out of Himalaya: the impact of past Asian environmental changes on the evolutionary and biogeographical history of Dipodoidea (Rodentia). *Journal of Biogeography* **42(5)**:856–870 DOI 10.1111/jbi.12476.

Pook CE, Joger U, Stümpel N, Wüster W. 2009. When continents collide: phylogeny, historical biogeography and systematics of the medically important viper genus *Echis* (Squamata: Serpentes: Viperidae). *Molecular Phylogenetics and Evolution* **53(3)**:792–807 DOI 10.1016/j.ympev.2009.08.002.

Popov SV, Akhmeteyev MA, Lopatin AV, Bugrova AM, Sychevskaya EK, Kopp ML, Szherba IG, Zaporozhets NI, Andreeva-Grigorovich AS, Nikolaeva IA. 2009. *Paleogeography and Biogeography of Paratethys Basin. Vol. I. Late Eocene–Early Miocene.* Moscow: Nauchny Mir, 200 [in Russian].

Popov SV, Rögl F, Rozanov AY, Steininger FF, Shcherba IG, Kovac K. 2004. *Lithological-Paleographic Maps of Paratethis. 10 Maps Late Eocene to Pliocene.* Frankfurt: Courier Forschungsinstitut Senckenberg, 46.

Prasad GVR, Bajpai G. 2008. Agamid lizards from the early Eocene of western India: oldest Cenozoic lizards from South Asia. *Palaeontology Electronica* **11**:1–19.

Qi Y, Yang W, Lu B, Fu J. 2013. Genetic evidence for male-biased dispersal in the Qinghai toad-headed agamid *Phrynocephalus vlangalii* and its potential link to individual social interactions. *Ecology and Evolution* **3(5)**:1219–1230 DOI 10.1002/ece3.532.

Rahiamian H, Shafiei S, Rastegar Pouyani N, Rastegar Pouyani E. 2015. Phylogenetic relationships of the gray-toad agama, *Phrynocephalus scutellatus* (Olivier, 1807), species complex from Iran. *Zootaxa* **3990(3)**:369–380 DOI 10.11646/zootaxa.3990.3.3.

Rambaut A, Drummond AJ. 2007. Tracer v1. 5. *Available at http://beast.bio.ed.ac.uk/Tracer.*

Ramstein G, Fluteau F, Besse J, Joussaume S. 1997. Effect of orogeny, plate motion and land-sea distribution on Eurasian climate change over the past 30 million years. *Nature* **386(6627)**:788–795 DOI 10.1038/386788a0.

Ree RH, Moore BR, Webb CO, Donoghue MJ. 2005. A likelihood framework for inferring the evolution of geographic range on phylogenetic trees. *Evolution* **59(11)**:2299–2311 DOI 10.1111/j.0014-3820.2005.tb00940.x.

Ree RH, Smith SA. 2008. Maximum likelihood inference of geographic range evolution by dispersal, local extinction, and cladogenesis. *Systematic Biology* **57(1)**:4–14 DOI 10.1080/10635150701883881.

Renner SS. 2016. Available data point to a 4-km-high Tibetan Plateau by 40 Ma, but 100 molecular-clock papers have linked supposed recent uplift to young node ages. *Journal of Biogeography* **43(8)**:1479–1487 DOI 10.1111/jbi.12755.

Renoult JP, Geniez P, Bacquet P, Benoit L, Crochet P-A. 2009. Morphology and nuclear markers reveal extensive mitochondrial introgressions in the Iberian Wall Lizard species complex. *Molecular Ecology* **18(20)**:4298–4315 DOI 10.1111/j.1365-294X.2009.04351.x.

Rögl F. 1998. Paleogeographic considerations for Mediterranean and Paratethys seaways (Oligocene and Miocene). *Annalen des Naturhistorischen Museums in Wien* **99A**:279–331.

Rögl F. 1999. Mediterranean and Paratethys. Facts and hypotheses of an Oligocene to Miocene paleogeography (short overview). *Geologica Carpathica* **50(4)**:339–349.

Ronquist F, Huelsenbeck JP. 2003. MrBayes 3: Bayesian phylogenetic inference under mixed models. *Bioinformatics* **19(12)**:1572–1574 DOI 10.1093/bioinformatics/btg180.

Sambrook J, Fritsch EF, Maniatis T. 1989. *Molecular coning: a laboratory manual. Second edition.* New York: Cold Spring Harbour Laboratory Press, 385 p.

Scherler L, Mennecart B, Hiard F, Becker D. 2013. Evolutionary history of hoofed mammals during the Oligocene-Miocene transition in Western Europe. *Swiss Journal of Geosciences* **106(2)**:349–369 DOI 10.1007/s00015-013-0140-x.

Shackleton RM, Chang C. 1988. Cenozoic uplift and deformation of the Tibetan Plateau: the geomorphological evidence. The Geological Evolution of Tibet. *Philosophical Transactions of the Royal Society* **327(1594)**:365–377.

Sharma RC. 1978. A new species of *Phrynocephalus* Kaup (Reptilia: Agamidae) from the Rajasthan Desert, India, with notes on ecology. *Bulletin of the Zoological Survey of India* **1(3)**:291–294.

Shenbrot G, Bannikova A, Giraudoux P, Quere JP, Raoul F, Lebedev V. 2017. A new recent genus and species of three-toed jerboas (Rodentia: Dipodinae) from China: a living fossil? *Journal of Zoological Systematics and Evolutionary Research* **55(4)**:356–368 DOI 10.1111/jzs.12182.

Shimodaira H. 2002. An approximately unbiased test of phylogenetic tree selection. *Systematic Biology* **51(3)**:492–508 DOI 10.1080/10635150290069913.

Shoo LP, Rose R, Doughty P, Austin JJ, Melville J. 2008. Diversification patterns of pebble-mimic dragons are consistent with historical disruption of important habitat corridors in arid Australia. *Molecular Phylogenetics and Evolution* **48(2)**:528–542 DOI 10.1016/j.ympev.2008.03.022.

Šmíd J, Carranza S, Kratochvil L, Gvozdik V, Nasher AK, Moravec J. 2013. Out of Arabia: a complex biogeographic history of multiple vicariance and dispersal events in the gecko genus *Hemidactylus* (Reptilia: Gekkonidae). *PLOS ONE* **8(5)**: DOI 10.1371/journal.pone.0064018.

Smit JHW, Cloetingh SAPL, Burov E, Tesauro M, Sokoutis D, Kaban M. 2013. Interference of lithospheric folding in western Central Asia by simultaneous Indian and Arabian plate indentation. *Tectonophysics* **602**:176–193 DOI 10.1016/j.tecto.2012.10.032.

Sokolovsky VV. 1975. Karyotypes and taxonomy of lizards of the family Agamidae. In: *Biologicheskiye Issledovaniya na Dalnem Vostoke.* Vladivostok: Nauka, 107–111 [in Russian].

Solovyeva EA. 2017. The position of *Phrynocephalus rossikowi* (Reptilia, Agamidae) according to mtDNA from old museum specimen. In: *SEH 19th European Congress of Herpetology. Programme and Abstracts*, University of Salzburg, 18–23 September 2017, 256.

Solovyeva EN, Dunayev EA, Poyarkov NA. 2012. Interspecific taxonomy of sunwatcher toadhead agama species complex (*Phrynocephalus helioscopus*, Squamata). *Zoologicheskiy Zhurnal* **91(11)**:1377–1396.

Solovyeva EN, Poyarkov NA, Dunayev EA, Duysebayeva TN, Bannikova AA. 2011. Molecular differentiation and taxonomy of the sunwatcher toad headed agama species complex *Phrynocephalus* superspecies *helioscopus* (Pallas 1771) (Reptilia: Agamidae). *Russian Journal of Genetics* **47(7)**:952–996 DOI 10.1134/s1022795411070155.

Solovyeva EN, Poyarkov NA, Dunayev EA, Nazarov RA, Lebedev VS, Bannikova AA. 2014. Phylogenetic relationships and subgeneric taxonomy of toad-headed agamas Phrynocephalus (Reptilia, Squamata, Agamidae) based on mitochondrial DNA sequence data. *Doklady Biological Sciences* **455**:119–124 DOI 10.1134/S0012496614020148.

Swofford DL. 2002. *Phylogenetic Analysis Using Parsimony (*and Other Methods)*. Version 4. Sunderland: Sinauer Associates.

Szczerbak NN. 2003. *Guide to the Reptiles of the Eastern Palearctic*. In: Golubev ML, Malabar: Krieger Publishing, 260.

Szczerbak [Shcherbak] NN. 1994. Zoogeographic analysis of reptiles of Turkmenistan. *Monographiae Biologicae* **72**:307–328 DOI 10.1007/978-94-011-1116-4_19.

Tamura K, Stecher G, Peterson D, Filipski A, Kumar S. 2013. MEGA6: molecular evolutionary genetics analysis version 6.0. *Molecular Biology and Evolution* **30(12)**:2725–2729 DOI 10.1093/molbev/mst197.

Terentjev PV, Chernov SA. 1949. *Opredelitel Presmykatushchikhsya i Zemnovodnykh [Field guide to reptiles and amphibians (in Russian)]*. Moscow: Cob. Hayka.

Thompson JD, Higgins DG, Gibson TJ. 1994. CLUSTAL W: improving the sensitivity of progressive multiple sequence alignment through sequence weighting, position-specific gap penalties and weight matrix choice. *Nucleic Acids Research* **22(22)**:4673–4680 DOI 10.1093/nar/22.22.4673.

Toews DPL, Brelsford A. 2012. The biogeography of mitochondrial and nuclear discordance in animals. *Molecular Ecology* **21(16)**:3907–3930 DOI 10.1111/j.1365-294X.2012.05664.x.

Townsend TM, Alegre RE, Kelley ST, Wiens JJ, Reeder TW. 2008. Rapid development of multiple nuclear loci for phylogenetic analysis using genomic resources: an example from squamate reptiles. *Molecular Phylogenetics and Evolution* **47(1)**:129–142 DOI 10.1016/j.ympev.2008.01.008.

Townsend TM, Mulcahy DG, Noonan BP, Sites JW, Kuczynski CA, Wiens JJ, Reeder TW. 2011. Phylogeny of iguanian lizards inferred from 29 nuclear loci, and a comparison of concatenated and species-tree approaches for an ancient, rapid radiation. *Molecular Phylogenetics and Evolution* **61(2)**:363–380 DOI 10.1016/j.ympev.2011.07.008.

Uetz P, Hošek J. 2016. The Reptile Database. *Available at http://www.reptile-database.org* (accessed 23 March 2016).

Urquhart J, Wang Y, Fu J. 2009. Historical vicariance and male-mediated gene flow in the toad-headed lizards *Phrynocephalus przewalskii*. *Molecular Ecology* **18(17)**:3714–3729 DOI 10.1111/j.1365-294X.2009.04310.x.

Wang Y, Fu J. 2004. Cladogenesis and vicariance patterns in the toad-headed lizard *Phrynocephalus versicolor* species complex. *Copeia* **2(2)**:199–206 DOI 10.1643/CG-03-082R1.

Wang YZ, Macey JR. 1993. On the ecologico-geographic differentiation of Chinese species of the genus *Phrynocephalus*. In: *Proceedings of the First Asian Herpetological Meeting*, 147.

Weise V. 1974. The slope development and plain formation in the deserts of the Iranian highlands. *Wurzburger Geographische Arbeiten* **24**:21–26.

Wermuth H. 1967. Liste der rezenten Amphibien und Reptilien. Agamidae. *Das Tierreich.* Vol. 86. Berlin: Walter de Gruyter.

Whiteman RS. 1978. Evolutionary history of the lizard genus *Phrynocephalus* (Lacertilia, Agamidae). M.A. Thesis. Fullerton: California State University, 113.

Xia X, Hu W. 1993. The resources and environment in the Taklimakan Desert. *Science in China (Series B)* **23**(8):889–896.

Yang Z. 2007. PAML 4: phylogenetic analysis by maximum likelihood. *Molecular Biology and Evolution* **24**(8):1586–1591 DOI 10.1093/molbev/msm088.

Yang SJ, Yin ZH, Ma XM, Lei FM. 2006. Phylogeography of ground tit (Pseudopodoces humilis) based on mtDNA: evidence of past fragmentation on the Tibetan plateau. *Molecular Phylogenetics and Evolution* **41**(2):257–265 DOI 10.1016/j.ympev.2006.06.003.

Yuan W, Carter A, Dong J, Bao Z, An Y, Guo Z. 2006. Mesozoic–Tertiary exhumation history of the Altai Mountains, northern Xinjiang, China: new constraints from apatite fission track data. *Tectonophysics* **412**(3–4):183–193 DOI 10.1016/j.tecto.2005.09.007.

Zachos J, Pagani M, Sloan L, Thomas E, Billups K. 2001. Trends, rhythms, and aberrations in global climate 65 Ma to present. *Science* **292**(5517):686–693 DOI 10.1126/science.1059412.

Zarza E, Reynoso VH, Emerson BC, Brent C. 2011. Discordant patterns of geographic variation between mitochondrial and microsatellite markers in the Mexican black iguana (Ctenosaura pectinata) in a contact zone. *Journal of Biogeography* **38**(7):1394–1405 DOI 10.1111/j.1365-2699.2011.02485.x.

Zeng XM, Wang YZ, Liu ZJ, Fang ZL, Wu GF, Papenfuss TJ, Macey JR. 1997. Karyotypes of nine species in the genus *Phrynocephalus*, with discussion of karyotypic evolution of Chinese *Phrynocephalus*. *Acta Zoologica Sinica* **43**:399–410.

Zerova GA, Chkhikvadze VM. 1984. The review of Cenozoic lizards and snakes in USSR. News. *Georgian SSR Academy of Sciences Series: Biology* **10**:319–325.

Zhang Q, Xia L, He J, Wu Y, Fu J, Yang Q. 2010. Comparison of phylogeographic structure and population history of two *Phrynocephalus* species in the Tarim Basin and adjacent areas. *Molecular Phylogenetics and Evolution* **57**(3):1091–1104 DOI 10.1016/j.ympev.2010.10.003.

Zhao EM, Adler K. 1993. *Herpetology of China.* Ithaca: Society for the Study of Amphibians and Reptiles.

Zhao EM, Zhao KT, Zhou KY. 1999. *Fauna Sinica. Reptilia. Vol. 2. Squamata. Lacertilia.* Beijing: Science Press, 394.

Zheng H, Wei X, Tada R, Clift PD, Wang B, Jourdan F, Wang P, He M. 2015. Late Oligocene-early Miocene birth of the Taklimakan Desert. *Proceedings of the National Academy of Sciences of the United States of America* **112**(25):7662–7667 DOI 10.1073/pnas.1424487112.

Zhisheng A, Kutzbach JE, Prell WL, Porter SC. 2001. Evolution of Asian monsoons and phased uplift of the Himalaya–Tibetan Plateau since late Miocene times. *Nature* **411**(6833):62–66 DOI 10.1038/35075035.